8-2010

FRICTION MEASUREMENT IN PRECISION GLASS MOLDING

Peiman Mosaddegh
Clemson University, p.mosadegh@gmail.com

FRICTION MEASUREMENT IN PRECISION GLASS MOLDING

A Thesis
Presented to
the Graduate School of
Clemson University

In Partial Fulfillment
of the Requirements for the Degree
Doctor of Philosophy
Mechanical Engineering

---

by
Peiman Mosaddegh
August 2010

Accepted by:
Dr. John Ziegert, Committee Chair
Dr. Paul Joseph
Dr. Michael Ellison
Dr. Lonny Thompson

ABSTRACT

Extensive growth of state-of-the-art technologies has created a demand for high quality lenses and has driven the industry toward an inexpensive process for manufacturing of aspheric glass lenses called Precision Glass Molding (PGM). Finite Element Analysis (FEA) has been used to predict the right mold geometry. Having a realistic simulation to predict mold geometry depends on the correct model of material behavior and friction coefficient at elevated temperature.

Finding the static and dynamic coefficient of friction experimentally between two flat surfaces at elevated temperature is the subject of this research. The equipment used in this study was originally designed for the Precision Glass Molding (PGM) process and was modified for friction measurement by using molds designed specifically for the friction test. The performance of this apparatus was validated using a steel-steel friction pair at room temperature and a steel-BK7 pair at elevated temperature.

The frictional behavior of two different types of oxide glasses; BK7 and Soda-Lime-Silica glass have been studied. During trials at which the temperature is above the glass transition temperature, the results show the effect of glass viscoelasticity in the friction data. This effect is in the form of exponential increase in friction force data prior to the onset of sliding. Moreover, the effect of stick-slip phenomenon can be seen as a jump in the position data (in the order of microns in tangential direction). Coulomb's Law has been used to calculate the friction coefficient. An average friction coefficient has been defined and calculated for some trials, providing a quantitative value for dynamic friction coefficient at different process parameters.

The final part of the investigation involved using the Design of Experiment approach to include a broader range of processing parameters and do a sensitivity analysis to find the effect of temperature, normal force, feed rate, and surface finish on dynamic friction coefficient.

The finding from the current investigation demonstrates reasonable changes in dynamic friction of glass due to its viscoelastic properties close to its transition temperature. These friction data can be used to improve the accuracy of simulations of the PGM process.

DEDICATION

I would like to dedicate this thesis and work to my dearest wife, Dr. Neda Yavari who has been a perpetual source of love, encouragement and motivation. To my parents, Mrs. Ashraf Rajaei and Mr. Hooshang Mosaddegh who have been my teachers in this world. To my daughter, Mahya Mosaddegh who has brought more meaning to my life. This thesis would not have been possible without their support.

ACKNOWLEDGMENTS

I would like to thank my advisor, Dr. John Ziegert for his guidance, and his endless support throughout the course of this project. Dr. Ziegert's constant feedback and high expectations have driven me to keep making progress and complete this work. I extend my sincere thanks to Dr. Kathleen Richardson for allowing me access to her lab.

My appreciation goes out to Dr. Paul Joseph, Dr. Michael Ellison and Dr. Lonny Thompson for serving on my committee and guiding me throughout my research experience. Each of you was very instrumental in the completion of my thesis and in developing my overall knowledge in the field of Mechanical Engineering and Material Science.

The successful completion of this thesis was possible due to technical support of Dr. Yazid Tohme from Moore Nanotechnology LLC. A special thanks to my fellow graduate students Vincent Lee, and Waqas Iqbal for their selfless help during the course of this work. I would also like to thank Dr. David Musgraves for helping me to understand glass behavior. Finally, I would like to thank my family and friends for all the love and care without which this work would be incomplete.

TABLE OF CONTENTS

Page

Table of Contents (Continued)

Page

Table of Contents (Continued)

LIST OF TABLES

LIST OF FIGURES

List of Figures (Continued)

List of Figures (Continued)

List of Figures (Continued)

Figure Page

CHAPTER ONE

INTRODUCTION

Introduction

Glass, an amorphous solid at room temperature, cools quickly during solidification. Since it doesn't exhibit a distinct melting or freezing point, it is characterized by a transition region from solid to super-cooled liquid called the glass transformation, or glass transition region (T_g). Figure 1-1 represents this behavior based on either enthalpy or volume for most glasses [1]. Also, this figure shows the fictive temperature (T_f), which is the artificial quantitative representation of deviation from equilibrium, and it depends on cooling rate.

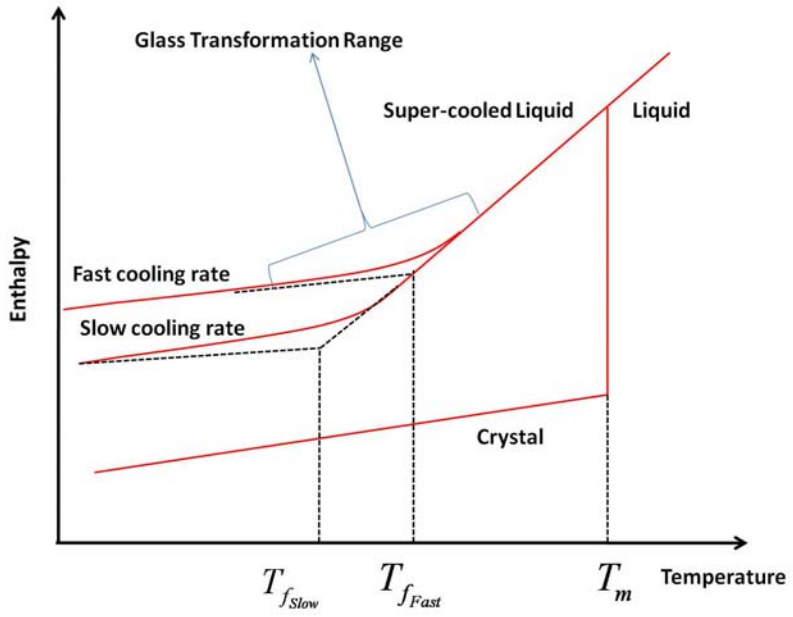

Figure 1-1: Typical enthalpy-temperature graph for glass material

At room temperature (below Tg), most commercial glasses are in the glassy state, their behavior being elastic and brittle [2]. When the temperature increases in the temperature range close to Tg, the glass softens, exhibiting viscoelastic behavior, which is temperature dependent.

At low viscosities when glass is significantly above Tg, hot glass gobs behave as viscous fluids, which immediately relax to relieve an applied stress, and at extremely high viscosity when glass is significantly below Tg, they respond to rapid application of a stress as if they were an purely elastic material. In other word, viscoelastic behavior, where the material behaves neither purely as an elastic solid, nor a purely viscous liquid, can be observed in glasses over a large temperature range.

The calorimetric glass transition lies within the viscoelastic temperature range, but the overlap of the two is determined by the viscosity-temperature curve of the glass, which is ultimately a function of composition.

1-1 Precision Glass Molding

Extensive growth of state-of-the-art technologies has created a demand for high quality lenses and has driven the industry toward an inexpensive process for manufacturing of aspheric glass lenses. Conventional abrasive methods such as CNC machining, grinding and polishing are suitable for producing spherical but not aspherical lenses. Precision Glass Molding (PGM) offers a cost-effective alternative for the mass production of these lenses. Moreover, this method is a green technology requiring no environmentally damaging coolant.

The PGM process includes three steps, heating, molding and cooling, as seen in Figure 1-2. First, the glass gob is inserted between the top and bottom molds at room temperature. During the heating process, its temperature increases above the transition temperature, deforming both the glass and the molds due to thermal expansion. During the compression (molding) step, the heated glass is pressed into the thermally deformed mold surfaces. Finally, in the cooling step both the glass and molds cool to room temperature and the final product is ready to be released. This entire process can be completed in less than 25 minutes.

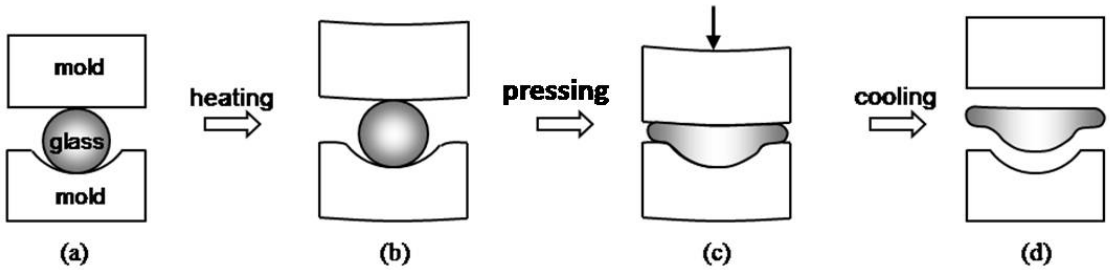

Figure 1-2: Precision glass molding process

Although in the cooling stage of the PGM process the molds recover their initial shapes, the final geometry of the glass is different from that of the molds due to thermal contraction. In addition, the cooling stage has the most significant effect on the residual stresses, a condition that also changes the final shape of the molded glass. The problem with the current PGM process is this final deformation of the glass, meaning the the deviation of the molded lens is not suitable for the aspherical lenses needed by today's sophisticated technologies.

A problem of equal importance is the cost of creating molds of the proper geometry to create lenses of the desired shape, a process accurately achieved by trial and error. To improve mold design and avoid these multiple iterations, Finite Element Analysis (FEA) has been used to predict the correct mold geometry; however, the use of this method has been the subject of limited research. Most researchers have used commercial FEA software such as DEFORM and ABAQUS in glass molding simulation. For example, Yi *et al.* [3] used DEFORM-2D to simulate the compression molding of aspherical glass lenses while Jian [4] investigated the numerical modeling of viscoelastic stress relaxation during the glass lens forming process using the non-linear FEM program, MARC, and Sellier *et al.* [5] used ABAQUS to develop an iterative algorithm for optical mold design. Klocke *et al*. [6] from the Fraunhofer Institute for Production Technology developed their own finite element code to simulate the PGM process.

Having a realistic simulation to predict mold geometry depends on the right model of material behavior at an elevated temperature, the appropriate value of heat flux between the surfaces the glass and the molds at a high temperature and pressure, the appropriate value of friction coefficient between surfaces at an elevated temperature, and the viscoelastic stress relaxation during the cooling step. Of these issues, friction has been the focus of the least extensive research. To address this need, this study proposes the dynamic and static friction measurement of glass at elevated temperatures.

1-2 Determination of Friction Coefficient

The ASTM document G 115, Standard Guide for Measuring and Reporting Friction Coefficient, explains different friction test methods for most solid materials at

room temperature based on the material and stiffness of the friction force measuring system.

1-3 Ring Compression Test

The ring compression test is a well-known method for measuring friction coefficients in the engineering science of metal forming process. Male and Sofuoglu [7, 8] developed this method, which is well-accepted today, to predict the friction coefficient in most metal forming processes. In this test, a ring with an initial defined dimension is plastically pressed between two flat platens. The change in the inner diameter and height of the final shape is used to determine the friction coefficient from a typical friction calibration curve. If the friction is high, the material flows inward and the inner diameter decreases, and if the friction is low, the material flows outward and the inner diameter increases. A schematic view of the effect of the friction magnitude on the metal flow in a ring compression test is shown in reference [8].

The calibration curves, which are calculated using FEA, are plotted for a wide range of friction coefficients in the literature and can be used directly for simulations in metal forming processes. In these types of calibration curves, the reduction in inner diameter and height can be used to find the friction coefficient.

The ring compression test is sensitive to material properties, surface condition, temperature, and strain rate, the latter two having the most significant impact. As Dawelski [9] has shown, the friction coefficient increases with increasing temperature in alloy steel. In addition, Wang *et al.* [10] found that the most significant parameter affecting the interfacial friction is the strain rate.

Similarly, the behavior of glass is also temperature dependant as the behavior of this material can range from elastic to viscoelastic to viscous based on its temperature. In addition, the surface roughness, material deterioration, and surface wear of the glass are affected by the temperature, in turn impacting the friction coefficient. As a result, the friction test should be conducted under application conditions. The next section contains a review of methods for friction measurement between hot glass (above T_g) and metal.

1-4 Kinetic Test to Measure the Friction Coefficient between Glass as a Viscous Material and Heated Metal

The effect of friction between glass as a viscous material and heated metal became important when researchers begin simulating the glass forming process 10 years ago. Hot glass exhibits elastic, viscoelastic, and viscous behaviors in different temperature ranges, meaning the resulting friction coefficient is across a range of temperature. An experimental method for addressing this problem has not yet been developed. This section reviews the current experimental methods for determining the friction coefficient of glass above its transition temperature.

Trier [11] was one of the first researchers who investigated the sliding behavior of hot viscous glass on metal surfaces, devising an experiment based on the kinetics of motion of a hot glass gob falling on a U-form circular path and then sliding through it.

In further investigations [12], he modified his apparatus to a rotary circular U-form channel made of metal. Then, he again measured the kinetics of motion of hot glass gob to calculate the friction between hot glass and metal.

This method is more accurate than the previous one because it measures more directly the friction coefficient, yet it is not sufficient because it does not consider the deformation energy inside the hot glass gob.

Recently, Falipou [13] developed another method for measuring the friction between hot viscous glass and metals considering the strain dissipation energy of a hot glass gob as it passes through a cylindrical funnel. He measured the speed of the glass gob at the exit of cylinder to determine its kinetic energy. The difference between the initial potential energy and this kinetic energy is the strain dissipation energy and friction loss. Using the principle of minimum energy for cylindrical funnel geometry, the associated dissipated energy was subtracted, resulting in the value of the friction loss.

These methodologies (Sections 1-2, 1-3, 1-4) suggest that to measure friction, the following considerations are necessary:

1- Because most PGM processes are performed close to the glass transition temperature, measuring friction in the viscoelastic behavior regime of glass is important.

2- Strain dissipation energy of a hot glass gob during the method used needs to be considered in the simulation.

3- The experiment should be similar to the conditions of the molding process to ensure similar material surface properties.

Although the ring compression test meets these conditions, it does not measure high friction coefficient values. Moreover, it is not an in-process method as it measures the ring dimensions only at the end of the test. As a result, another methodology is

necessary to obtain accurate test results, one that focuses on the dynamic rather than the static characteristics.

1-5 A Method for the Characterization of Friction during the Demolding of Microstructures Molded by Hot Embossing

A study conducted by Wrogull *et al.* [14, 15] investigated the determination of friction of microstructures of polymeric materials using a modified tensile testing machine that resembles the hot embossing process during the demolding stage. The advantage of this method is its similarity to the actual process, the results being more reliable than the ring compression test especially for FEA simulation. A schematic view of this machine is shown in Figure 1-3, and the resulting typical measurement curves for friction are shown in Figure 1-4. In this method, two planar polymeric samples are placed between two heating elements and a metal specimen. Also, this apparatus is equipped with two force transducer sensors, one for measuring the normal force and the other, the embossing force; thus, both static and dynamic friction can be measured based on Coulomb's law:

$$\mu_{stat} = F_{stat} / F_A \qquad \text{Eqa. (1.1)}$$

$$\mu_{dyn} = F_{dyn} / F_A \qquad \text{Eqa. (1.2)}$$

where F_{stat} is the static friction force measured by the machine, F_{dyn} the mean dynamic friction force measured by the machine, and F_A the normal force between the tool and the polymer.

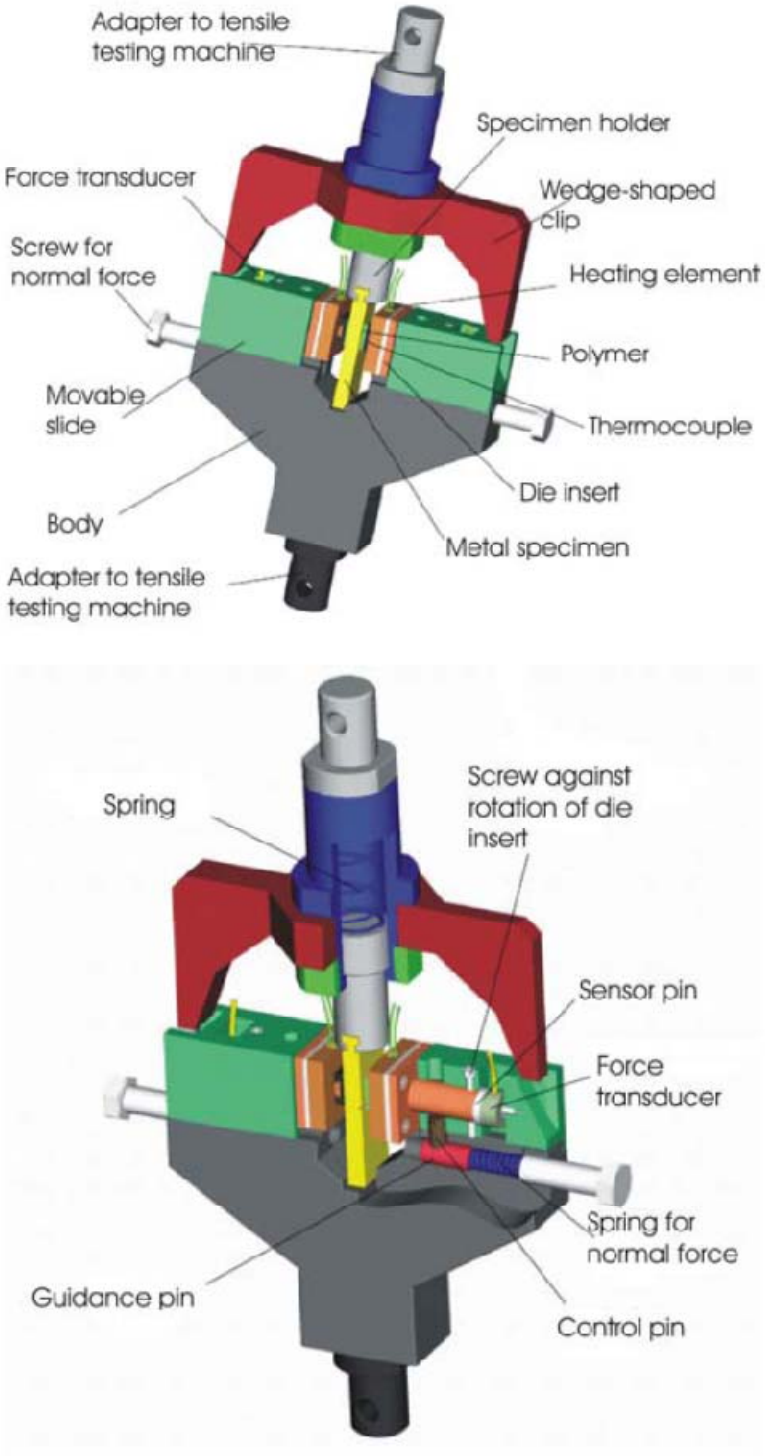

Figure 1-3: Schematic view of Worgull's apparatus for measuring friction -permission to duplicate the figure was given by the corresponding author [14]

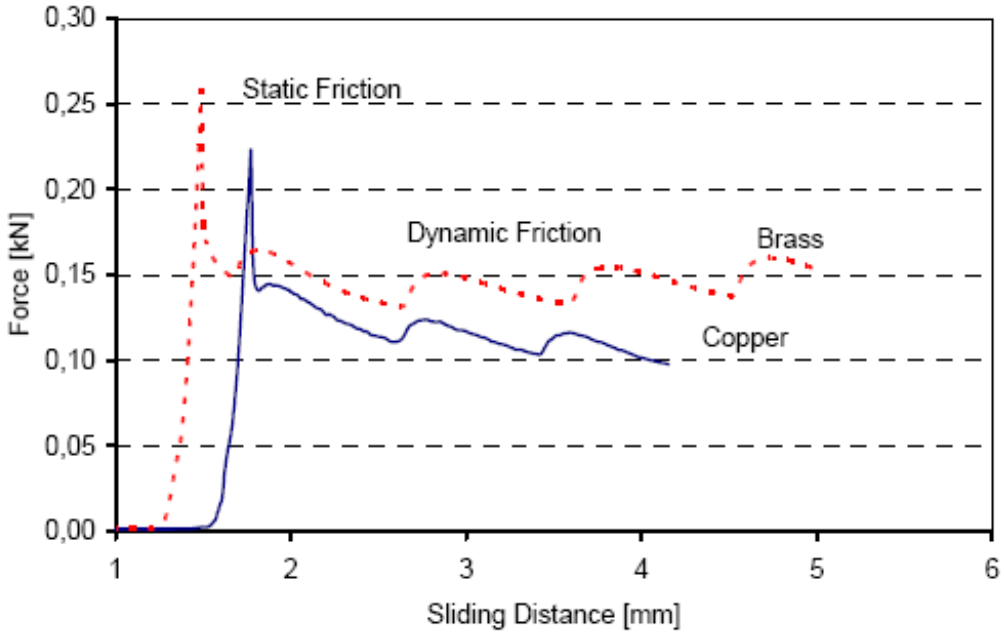

Figure 1-4: Typical friction force measurement between molded polymer and metal-Permission to duplicate the figure was given by the corresponding author [14]

This method can also be applied to glass because the processes for precision glass molding and hot embossing are similar. In both processes, the material is heated close to its transition temperature, then pressed between upper and lower mold dies and finally demolded below its transition temperature.

The concept behind this novel method to investigate the friction between hot glass and metal, as shown in Figure 1-5 is modified and described in detail in Chapter 3. In this modified method, two glass pieces with the desired surface finish are placed between metal molds and the normal force applied through adjustable springs attached to a load cell. Then, the metal mold which is heated to a finite value moves under position control (with finite feed rate) and simultaneously the pushing force (sliding force or friction force) is recorded through the PGM machine force transducer. Using the friction and

normal forces, the instantaneous friction coefficient will be calculated using the equation below:

$$\mu = \frac{F}{N} \qquad \text{Eqa. (1.3)}$$

where F is the friction force and N the normal force. The value of friction force versus the displacement of the glass gives the static and dynamic friction coefficient. Since this experimental method is similar to the molding environment, the results are more reliable than the ring compression test. This modified friction measurement will be discussed in further detail in Chapter 3.

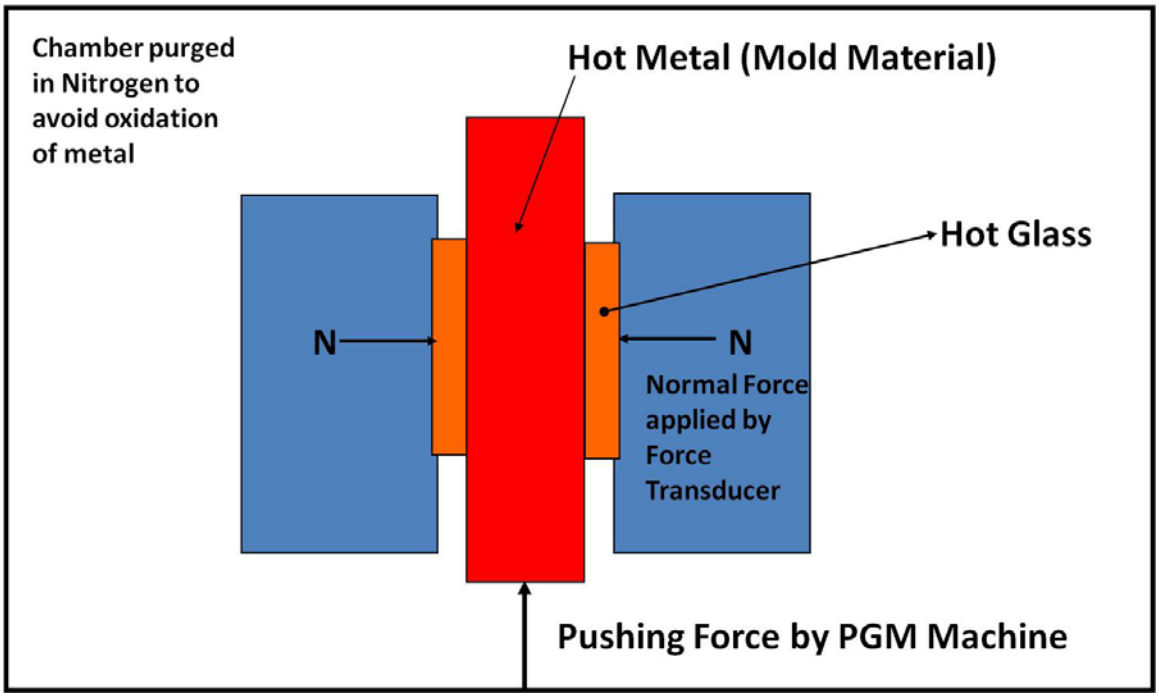

Figure 1-5: A schematic view for measuring the friction of hot glass using a PGM process

1-6 Outline

This thesis is organized as follows: Chapter 2 explains the motivation for this research, and the methodology and design of experiments are described in Chapter 3 while Chapter 4 discusses the material and methods. Experimental results are presented in Chapter 5, followed by observation and discussion in Chapter 6. Finally, the conclusions and future challenges regarding the modeling of the friction measurement are introduced in Chapters 7 and 8, respectively.

CHAPTER TWO

RESEARCH MOTIVATION AND OBJECTIVE

2-1 Motivation

The PGM process for molding glasses requires contact between the mold (metal) and the work piece (glass). As a result of this contact, sliding frictional forces are generated at the interface between the glass/mold surfaces. These friction forces affect the glass-forming process as they resist the relative movement of both materials. If this friction is strong, sticking overcomes sliding, resulting in shearing inside the glass. If the friction force is a weak, sliding occurs, and the glass deforms easily. To define these friction forces in PGM, there is a need to accurately determine the value of the friction coefficient between the glass and the mold under the molding condition. However, past research in the measurement of this friction force between hot glass and hot metals in the PGM process is limited. Even though some work has focused on the effect of glass as a lubricant in the ring compression test [8, 16], none has utilized this material as a sample in the test. In addition, studies considering the viscoelastic behavior of glass in the friction measurement for PGM simulation are limited. As a result, past FEA research used an arbitrary value for the friction coefficient.

For example, Jian and Yi [3, 17] arbitrarily used a friction coefficient of $\mu=0$ for the frictionless condition and $\mu=1$ for the sticking condition in their simulation of PGM. In another work [18], they used a friction coefficient of 0.5 to represent a true stick-slip friction model available in MARC. Although Klocke *et al.* [6] reported that the friction

needs to be defined as an input in the FEA software, they have not reported the value they used. Sellier *et al.* [5] also used an arbitrary value for the friction coefficient in their simulation, their results indicating that interface friction is an important factor in PGM and to model the deformation process, it is necessary to quantify this value accurately.

2-2 Objectives

To address the need for improved friction data, this research will focus on determining the friction coefficient between the glass and the mold material at elevated temperatures. Since glass behavior changes with temperature and load, its friction behavior may also change. Specifically, the goal in this study is to develop a method for experimentally measuring the dynamic and static friction between the glass and mold materials at temperatures close to the transition regime.

In addition, sensitivity analysis of various mold materials and process parameters (load and temperature) will be conducted to determine which has the most significant impact on the friction coefficient. Figure 2-1 illustrates the placement of this proposed study in relation to the PGM process.

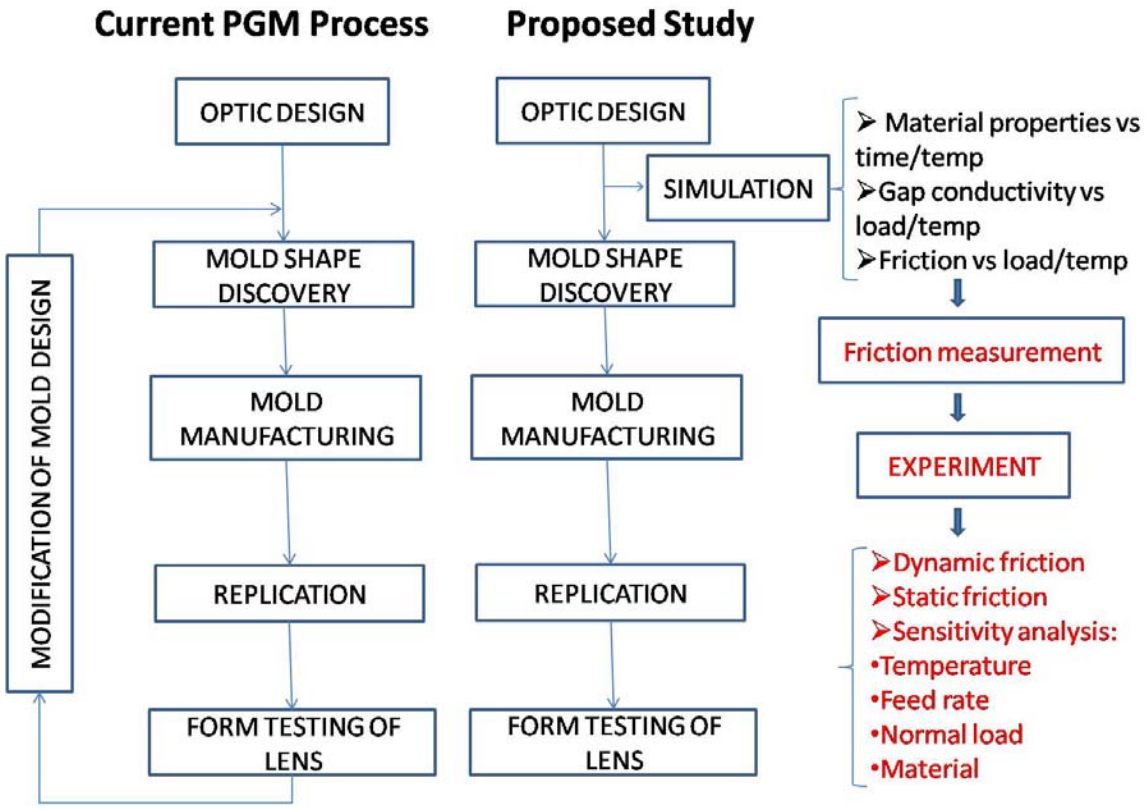

Figure 2-1: Placement of this research in the PGM process

CHAPTER THREE

METHODOLOGY AND DESIGN OF EXPERIMENT

3.1 Introduction

Since there is no data reported on the frictional behavior of glass used for PGM, it is necessary to measure friction experimentally under conditions similar to those used for this process. The equipment used in this study includes the PGM machine, molds designed specifically for this experiment, force transducers measuring normal and sliding forces, and data acquisition equipment. In this chapter, after the functionality of PGM machine is described, the experimental setup for the friction measurement is discussed.

3.2 PGM Machine

The machine used here, originally designed and manufactured by Moore Nanotechnology Systems LLC [19] for use in the PGM process, enables accurate control of the position, force, and temperature of the process. As the schematic side view in Figure 3-1 shows, the PGM machine is comprised of three main elements:

1- The lower base which includes the lower mold chamber, the push rod attached to a leadscrew driven by a servomotor, and a cylindrical glass tube outside the lower mold chamber. The cylindrical glass tube is raised and lowered outside the lower mold chamber using the two air cylinders installed on the bottom of this glass tube. When the glass tube is raised, the molding environment is isolated from the room conditions as the chamber is closed, and the interior can be filled with an inert gas or other gas such as nitrogen to prevent oxidation of the mold surfaces.

2- The upper base which includes the upper mold chamber, the force transducer, and the copper tubing connecting the mold chamber to the induction heating system unit.

3- The induction heating system (IHS) which is used to heat the mold and glass sample under test.

A drawing of the mold chamber assembly is shown in Figure 3-2 and a detailed cross-section drawing of the entire assembly is seen in Figure 3-3.

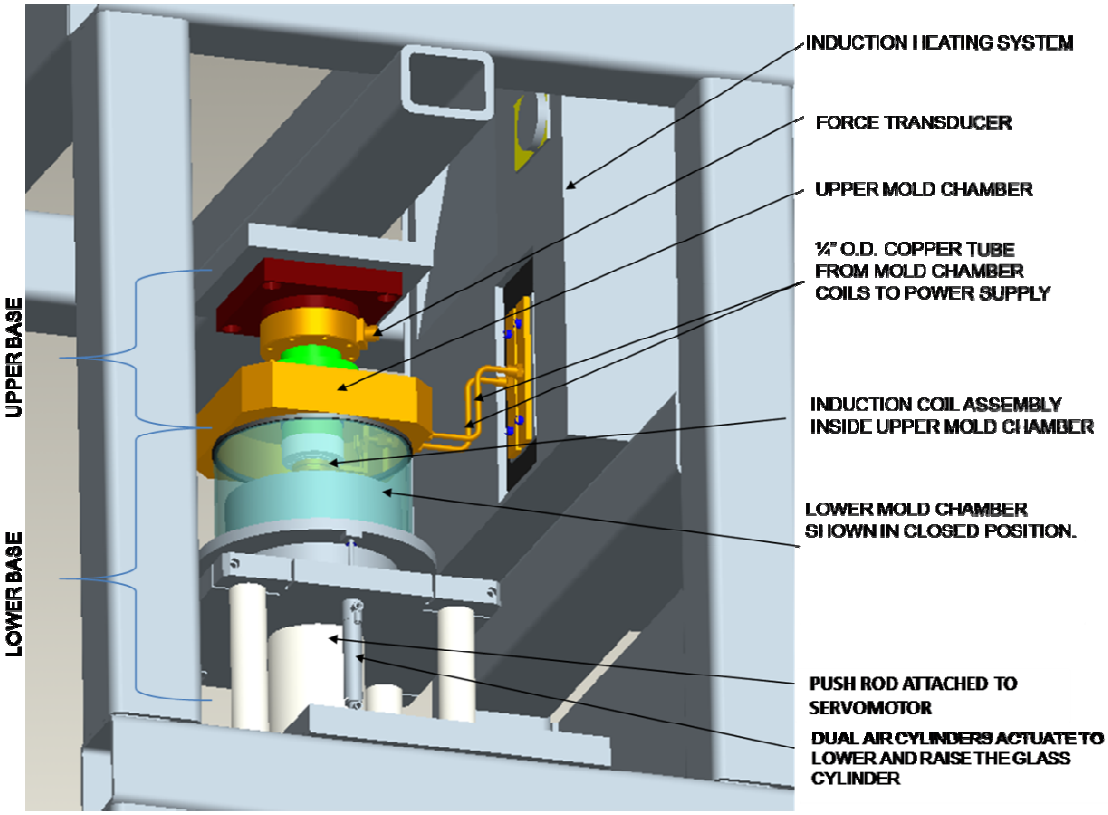

Figure 3-1: Schematic side view of the PGM machine (Moore Nanotechnology LLC. [19])

As Figure 3-2 shows, the machine uses an induction coil for the heating of the molds and glass. Using a strong AC magnetic field, this coil generates eddy currents in

the tungsten carbide molds. Resistance to these currents leads to the heating of the molds inside the coil. The advantage of this heating system is its fast heating cycle: the outer surfaces of the molds can reach temperatures of 500˚C in less than 10 seconds. A controller using two thermocouples as feedback sensors, one inside the top mold and the other inside the bottom mold, controls the temperature of the system during the heating, soaking, and pressing cycles. If the temperature exceeds the specified value, the induction heating stops. Also, nitrogen gas is pumped inside the chamber to help cool the molds during the cooling stage. A regulator valve controls the flow rate of nitrogen based on the temperature reading of the thermocouples.

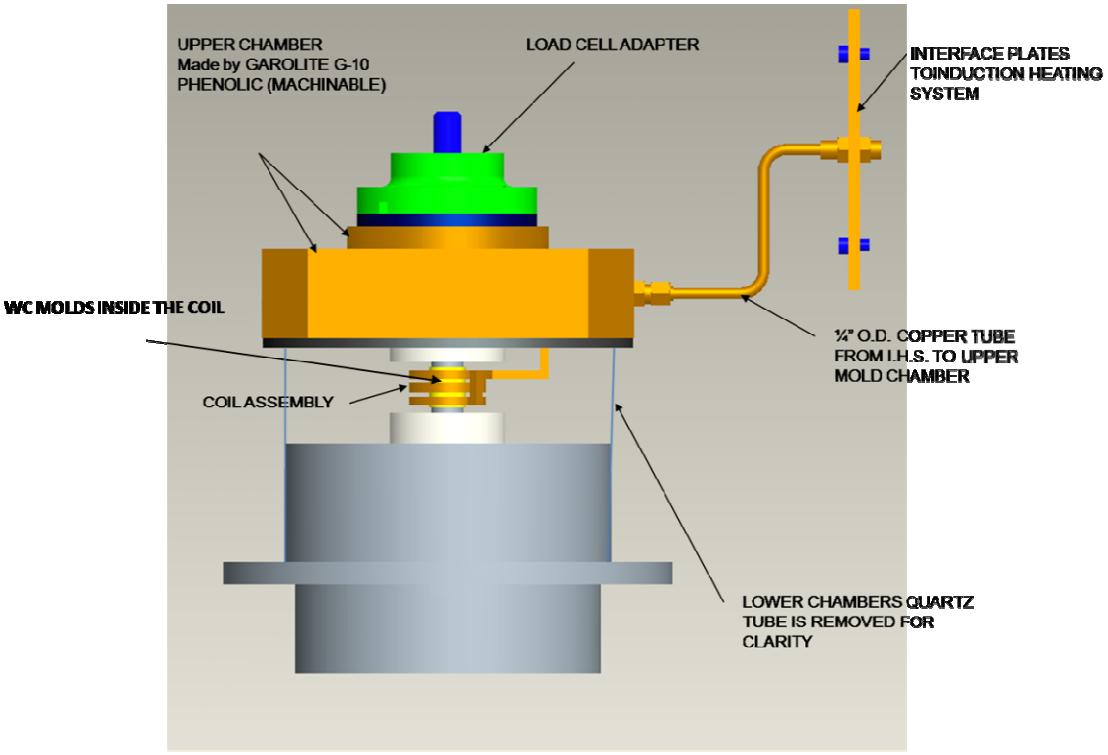

Figure 3-2: Mold chamber assembly (Moore Nanotechnology LLC. [19])

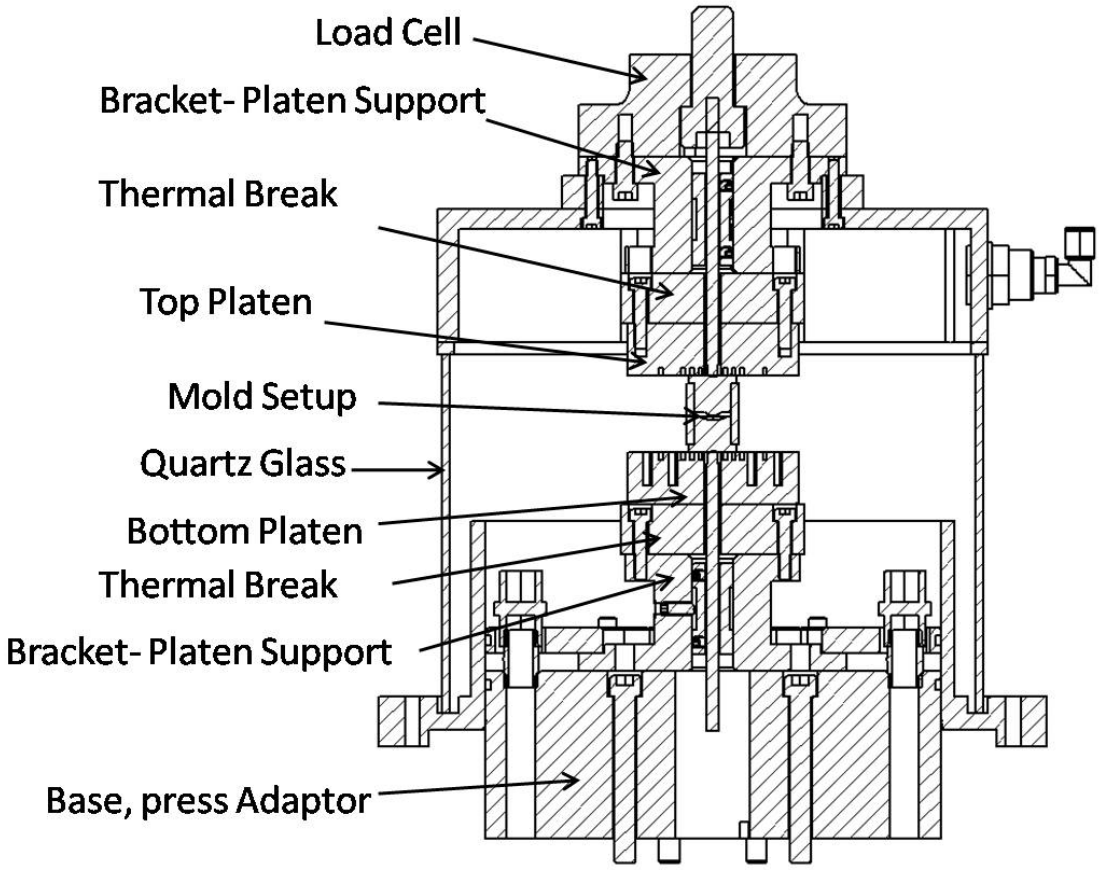

Figure 3-3: Mold chamber cross-section drawing (Moore Nanotechnology LLC. [19])

The drive system under the lower mold chamber includes a servomotor, gearbox, coupling, and ball screw as shown in Figure 3-4. This system has two modes of operation: position control and force control. A rotary encoder provides a feedback signal to the controller, monitoring the position control mode, and an inline load cell installed on the top of the upper chamber provides feedback during the force control mode of the machine as shown in Figure 3-2.

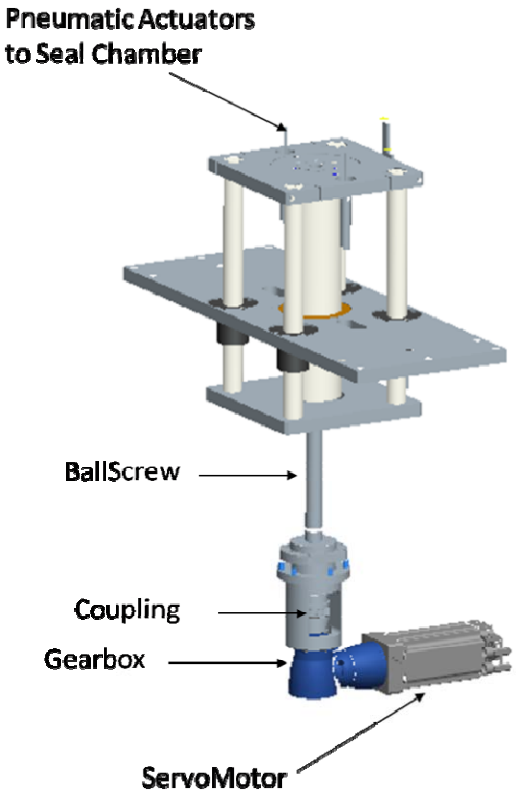

Figure 3-4: Drive system mechanism (Moore Nanotechnology LLC. [19])

3-2-1 Machine Functionality

Although the machine can operate using a variety of molds, the process remains essentially the same. First, a glass gob is seated between the top and bottom molds aligned by a cylindrical sleeve, and this entire assembly is installed between the upper and lower mold chambers. The temperature, force, and position profiles versus time are then defined for the molding process, and the chamber closes and is evacuated before being backfilled with nitrogen to remove the oxygen inside. A small flow rate of nitrogen gas will continuously purge inside the closed chamber to prevent the heated mold

surfaces from oxidation during the process. An exhaust tube is attached to the chamber to ventilate the nitrogen during the process.

The PGM process can be divided into the five steps below:

I. Heating step: The glass gob and the top and bottom molds heat to a specified temperature.

II. Soaking step: The temperature of the molds is kept constant until the temperature of glass reaches equilibrium.

III. Pressing: The glass is pressed after reaching the equilibrium temperature under either force or position control.

IV. Annealing or the first cooling step: Nitrogen gas flows into the chamber, cooling it at a specified rate. This cooling stage has a strong effect on the residual stresses and the final shape of the molded optic.

V. Fast cooling or the second cooling step: The final step of the process cools the entire setup to less than 200˚C to enable demolding.

3.3 Mold Design for Friction Test

To measure the friction forces versus displacement and determine the friction coefficient, the PGM machine was modified to collect data on such material properties as friction, gap conductivity, and the viscoelastic behavior of glass at elevated temperatures. The focus of this research is on the friction measurement.

To conduct friction measurements at elevated temperatures required both molds (mold setup) as shown in Figure 3-3 to be modified and then manufactured. The design has two parts: top and bottom mold. The top mold was installed in the upper mold

chamber and the bottom mold in the lower mold chamber. However, unlike conventional molding, the new upper and lower portions were designed so that the contact surface between the samples under test are in the vertical plane and parallel to the actuation direction of the machine's actuator, which will be used to cause relative sliding motion between them. Separate systems are provided to create a constant normal force between the sliding surfaces. To insure balanced loading, the apparatus was designed to simultaneously test two samples arranged 180˚ apart on the upper mold.

This modification process was governed by the considerations listed below:

I. The environment around the molds should be the same for both the friction test and the PGM process.

II. Both the glass and molds are heated using the same temperature profile of the PGM process (heating, soaking, and pressing).

III. The sliding friction force is collected by the load cell on the PGM machine while the normal force is measured using separate load cell and data collection equipment to ensure independent control of all applied forces.

IV. The apparatus must be designed to ensure that the maximum safe temperature of 93˚C for the force transducer is not exceeded.

V. The design should consider all geometrical limitations of the PGM machine and enable the friction apparatus to be installed completely inside the glass chamber.

Based on these requirements and constraints and using SOLIDWORK and ABAQUS, the components of the friction test apparatus were designed as shown in Figure 3-5 and Figure 3-6 for the top and bottom molds, respectively. As Figure 3-5

shows, the top mold includes a fixture holding the metal mold sample. An induction coil surrounds the upper cylindrical part of the mold that is attached to the top platen by six Inconel screws.

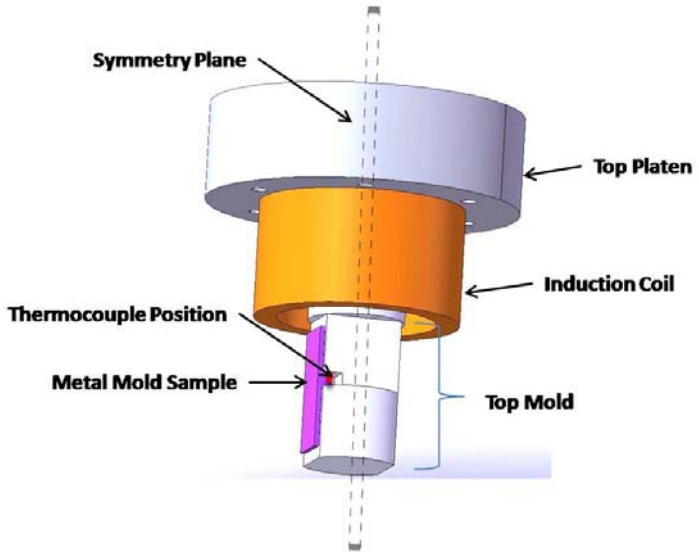

Figure 3-5: Top mold assembly

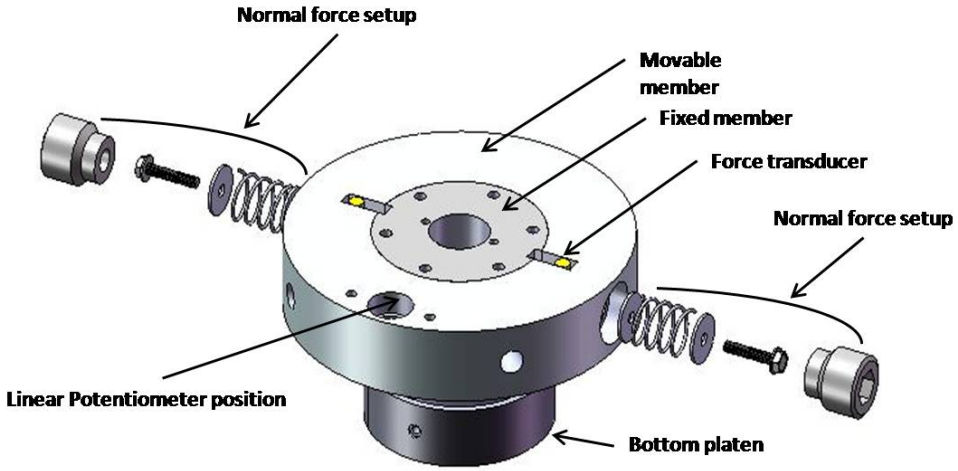

Figure 3-6: Bottom mold assembly

The bottom mold consists of a fixed and a movable part to guarantee easy attachment and alignment of the sample and measurement equipment, i.e. the glass piece, thermal insulator, and force transducer, inside the assembly. The former is attached to the bottom platen with the movable member encircling it. The movable member is seated after inserting the friction measurement equipment. Finally, a washer, spring and set screw are attached to the movable fixture to guarantee the perpendicular alignment of the entire system. Normal forces between the samples under test are measured by two miniature load cells that are loaded through a spring and adjusting screw assembly. A linear potentiometer (not shown in the figure) is attached to the movable fixture to measure the displacement between the bottom mold and the top mold which is fixed. A section drawing of this assembly is shown in Figure 3-7.

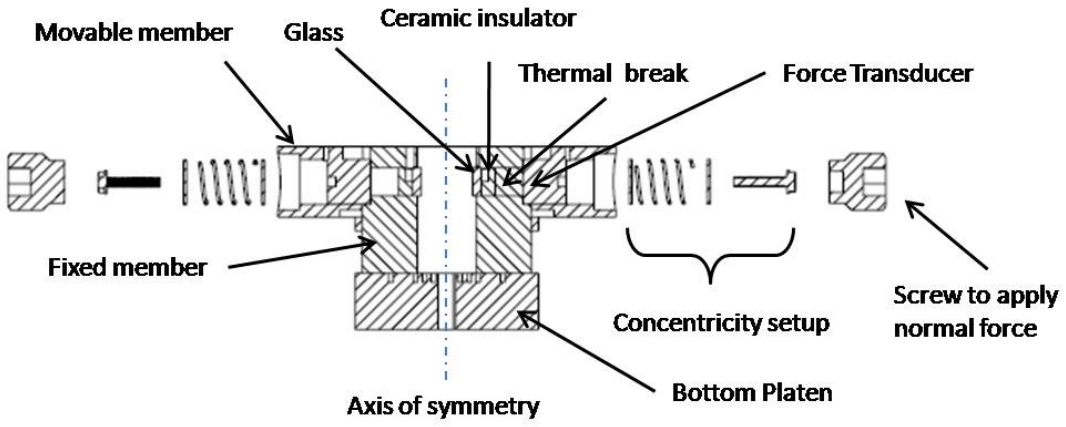

Figure 3-7: Cross-section view of Figure 3-6 showing the assembly of bottom mold

3.4 Material Selection for Top and Bottom Molds

In friction measurement at elevated temperatures, the materials were selected based on their thermal conductivity, a material property that describes the flow of heat

through a material at steady-state, and their thermal diffusivity, a property indicating how fast heat can move along the material in transient state. In addition, since this system relies on induction heating over a short period of time Inconel and Tungsten Carbide (WC) are good choices for the top mold. The selection of the material was defined by simulation to avoid any unpredictable temperatures in the top mold during the friction test.

In the real PGM operation, the temperature controller applies power to the induction coil whenever the temperature is less than the defined value of the desired temperature profile. When the temperature reaches the defined value, it then stops heating, and if the temperature rises above the target value, a nitrogen flow cools the system to maintain the temperature close to the target. As this loop continues, the error tends to decrease over time as the entire system reaches equilibrium.

To determine the right material for the top mold, a commercial FEA software ABAQUS was used to simulate the transient temperature behavior of the top mold. The 3D geometrical model of this simulation shown in Figure 3-8 illustrates the boundary condition of loading. In this system, the induction coil heating was modeled as a 1 KW surface heat flux into the cylinder of the fixture with the remaining surfaces, except the top surface which is insulated, allowing the heat to dissipate through forced convection. Two thermocouples detect the temperatures in the upper and middle surfaces of the part.

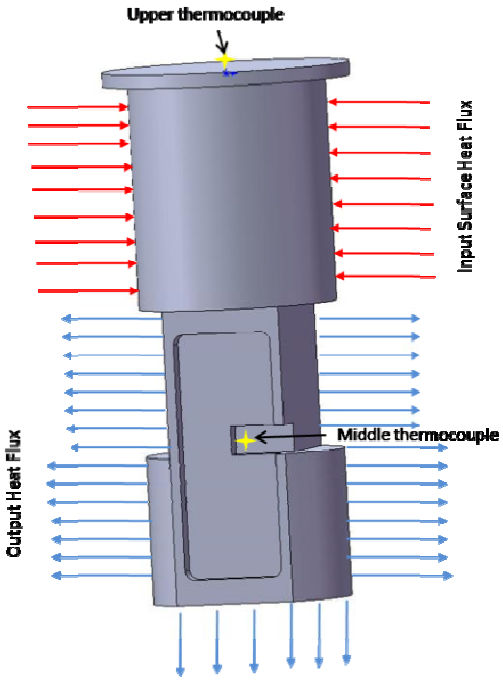

Figure 3-8: 3D view of boundary condition for simulation of heat transfer in upper fixture

The material properties and process parameters used in this simulation are shown in Table 3-1. Using a target temperature of 600˚C for the middle thermocouple, the results of the simulation at the middle and upper thermocouples for Inconel and WC are illustrated in Figure 3-9 and Figure 3-10, respectively.

Table 3-1: Parameters used in the simulation

Material	Thermal Conductivity (W/m˚C)	Specific heat (J/Kg˚C)	Density (Kg/m^3)	Film coefficient (W/m^2 ˚C)	Room temperature (˚C)	Target temperature (˚C)
Inconel	12.6	431	8280	100	20	600
WC	78.7	209	14650	100	20	600

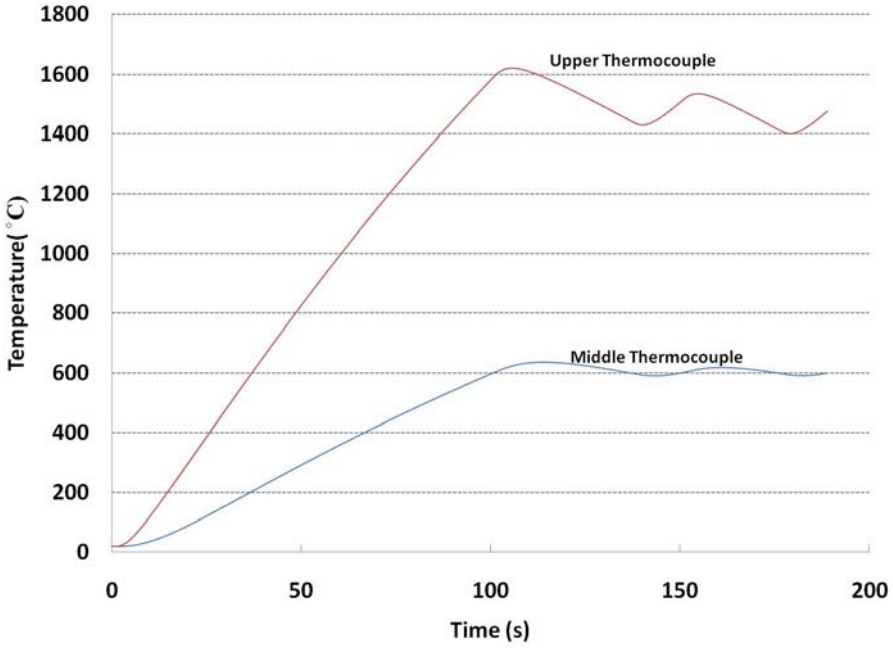

Figure 3-9: Temperatures at the middle and upper thermocouples for Inconel

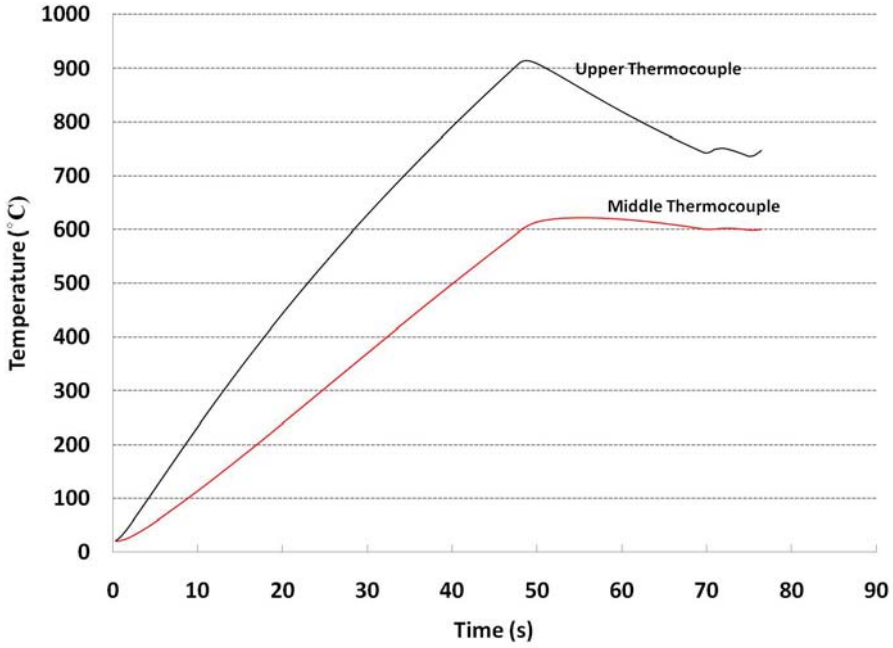

Figure 3-10: Temperatures at the middle and upper thermocouples for WC

The results of the simulation reveal that the temperature in WC reaches equilibrium (600˚C) twice as fast as for Inconel. In addition, the upper thermocouple temperature for Inconel reaches more than 1400˚C, which is very close to its melting temperature. Consequently, WC has been selected as the material for the top mold setup.

For the bottom mold, the only concern is that the temperature in the vicinity of the force transducer, as its maximum safe temperature is 93˚C according to the supplier's manual. Using a ceramic thermal break of 18 mm between the hot glass and the force transducer assures that the temperature around the transducer is in the range of the safe zone. As a result, the bottom mold setup can be made from a typical stainless steel such as SS304.

3.5 Experimental Setup

The experimental setup for the measurement of the frictional and normal forces is shown in Figure 3-11. After installation of the upper and lower molds and the test samples, the glass cylinder is raised into position to surround the molds and seal them from the exterior atmosphere. The chamber is evacuated and then filled with nitrogen to prevent the mold components from oxidation. The friction force was measured by the load cell (SWP-5K from Transducer Techniques Inc.) in the upper frame of the PGM machine, while the normal forces were measured by two mini-column load cells (MLC-2K from Transducer Techniques Inc.). These strain-gage-based force transducers can operate at temperatures up to 93˚C. To insure the safety of the load cells during high temperature testing, a ceramic insulator is placed between the load cell and the glass sample under test. The output from the load cells was a voltage signal conditioned and

amplified by a TMO-2 signal conditioning module purchased from the same company and received by a NI PCI-6229 data acquisition card. The resulting force data were then recorded using National Instruments Lab View graphical programming software. Both force signals and elapsed time were recorded for each run at a sampling frequency of 50 Hertz.

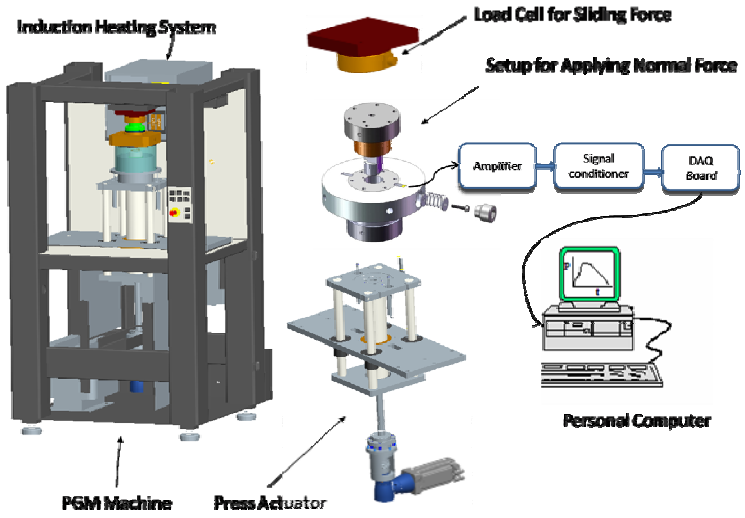

Figure 3-11: Experimental setup for friction measurement

The procedure for running the friction test is summarized below:

1- After the fixed member was installed on the bottom platen, the force transducer was inserted into the movable member through its slot guide and then placed on the top of bottom platen. Then the glass which is glued to ceramic piece is placed through its guide in the fixed member.

2- After installing the top mold, the fixed member of the bottom mold was moved upward toward the top until the sample to be tested was 20 mm inside the bottom mold.

3- Finally the normal force is applied by the screw. The washer and spring guarantees the perpendicular alignment of the whole setup.

4- Temperature and position profiles were created on the Graphical User Interface (GUI) of the PGM machine; a typical machine cycle for this test is shown in Figure 3-12. The temperature cycling seen is due to the on/off operation of the induction coil as it attempts to maintain the commanded temperature.

5- The machine began its cycle under position control, and all force transducers measured the force data. The linear potentiometer measures the relative displacement between the top and bottom molds.

6- Having determined both the frictional and normal forces, the instantaneous friction coefficient is calculated by $\mu = \frac{F}{N}$

where F and N are instantaneous friction and normal forces, respectively.

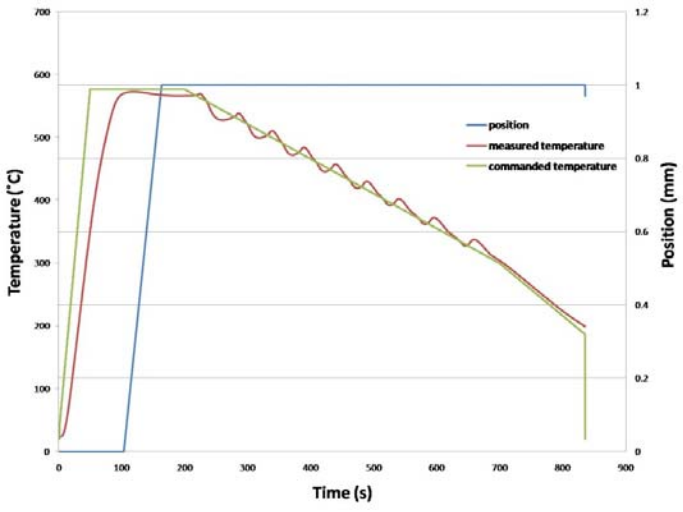

Figure 3-12: Typical temperature and position profile for friction test

CHAPTER FOUR

MATERIAL AND METHODS

4.1 Glass Material

Two types of oxide glasses are used in this research, N-BK7 (from SCHOTT Inc.) which is suitable for PGM process and soda-lime-silica glass (Optifloat from PILKINGTON Inc.) which is used in most of the literature. Both glasses are categorized as oxide glasses as the dominant part of their structure are comprised of silicon dioxide. The glass transition temperature (Tg) of both glasses is close, but their viscoelastic response is different away from Tg as their viscosity curve versus temperature behaves differently. In order to understand the glass viscoelasticity, the viscosity response of glass with respect to temperature needs to be understood.

4.1.1 Glass Viscosity

Glass is an inorganic polymer, held together with both covalent –Si-O-Si- bonds and ionic bonds. Its properties are temperature dependent, exhibiting non-linear behavior at elevated temperatures. For example, under high shear stress, much glass forms melts similar to polymers, exhibiting shear thinning behavior. A typical viscosity-temperature curve for soda-lime-silica glass in a wide range of temperature is shown in Figure 4-1. As this figure shows, the temperature of 550˚C is the glass transition temperature for this material.

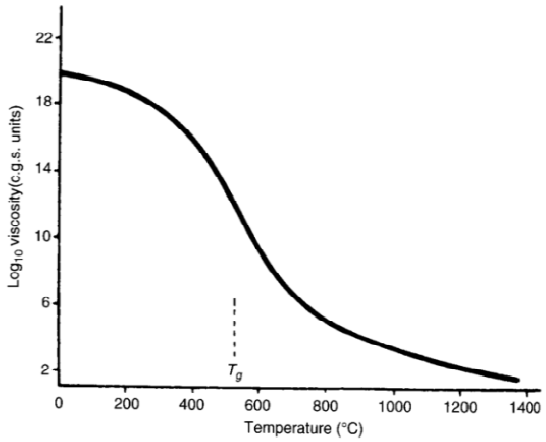

Figure 4-1: Viscosity-temperature relation of a soda-lime-silica glass [20]

The formation of glass objects from a melt requires accurate control of viscosity during the forming process as it depends on shear rate and temperature. According to Shelby [1], a number of specific viscosities based on NIST standard No. 710 have been selected as a reference point for most commercial glasses in the molding industry as illustrated in Figure 4-2.

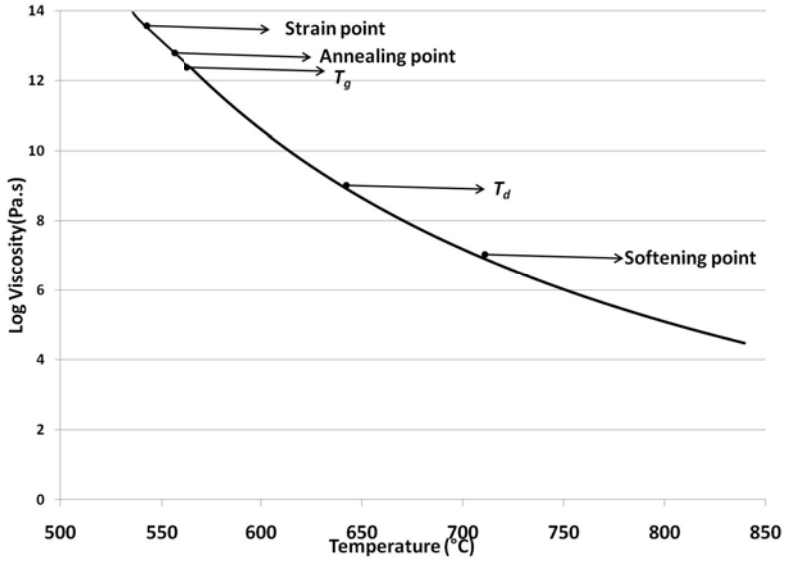

Figure 4-2: Reference point viscosity as a function of temperature for a soda-lime-silica glass melt

These reference points are defined as follows:

1- Melting point is a temperature at which the fining and homogeneity can be obtained in a reasonable time. The viscosity of melting point is <= 10 Pa.s for commercial glass.

2- Working point is the temperature at which the viscosity is approximately 10^3 Pa.s. This is the viscosity of glass for initial processing.

3- Softening point is a temperature at which the viscosity is close to $10^{6.6}$ Pa.s. At this viscosity, the glass melt stabilizes and does not deform under its own weight. The temperature range between the working and softening point is called the working range.

4- Annealing point is a temperature at which internal stress is relieved in a few minutes. The viscosity of a glass is between 10^{12} and $10^{12.4}$ Pa.s in this region.

5- Strain Point is a temperature at which internal stress is relieved in several hours. The viscosity of a glass is $10^{13.5}$ Pa.s, and it behaves as an elastic material in this region.

There are two other reference temperatures that are not used to show the viscosity of glass melt; the glass transition and dilatometric softening temperature can be easily used to compare the viscosity of different glass compositions during the glass forming process. The glass transition temperature, T_g, defined as the temperature at which the thermal expansion coefficient changes, depends upon the thermal mass (sample size), rate of heating, and property measured (thermal expansion, specific volume, enthalpy). As a result, different suppliers may report different values of T_g for the same glass, but an

average viscosity of $10^{12.3}$ Pa.s is reported by Moynihan [21] for common glasses. The dilatometric softening point, T_d, is the temperature at which the sample reaches its maximum length in a length versus temperature curve during the heating of the glass. It also depends on the applied load and the size of the sample.

The discussion above shows that glass melt behavior ranges from elastic to viscous depending on the temperature. In the other words, at low viscosities, hot glass gobs behave as viscous fluids and at extremely high viscosity, the super-cooled liquids show elasticity. There is an intermediate region in the viscosity-temperature curve where the response of these melts to applied stress lies between a pure liquid and an elastic solid, and is the called viscoelastic region. For common rates of stress application, these viscosities lie in the region of the glass transformation range, particularly in the range from 10^{13} to 10^{8} Pa.s.

In this study, the viscosity value at different temperatures is given by the suppliers and listed in Table 4-1. Based on these values and fitting (non-linear) them to the Vogel-Fulcher-Tammann (VFT) equation given by Equation (4.1) [22], the viscosity curves versus temperature for these two glasses are calculated and shown in Figure 4-3.

$$\mathrm{Log}(\eta) = A + \frac{B}{T - T_0} \qquad \text{Eqa. (4.1)}$$

where $\eta$is the viscosity at temperature T, and A, B, and T_0 are constants.

Table 4-1: Reference temperature for BK7 and Soda-Lime-Silica glass reported by supplier ($Pa.S$)

Glass type	Strain point	Transformation Temperature	Annealing Point	Softening Point
BK7	$log(\eta) = 13.5$ At Temp 557°C	$log(\eta) = 12$ At Temp 557°C	Not reported	$log(\eta) = 6.6$ At Temp 719°C
Soda-lime	$log(\eta) = 13.5$ At Temp 526°C	$log(\eta) = 12.3$ At Temp 552°C	$log(\eta) = 10.3$ At Temp 600°C	$log(\eta) = 6.6$ At Temp 732°C

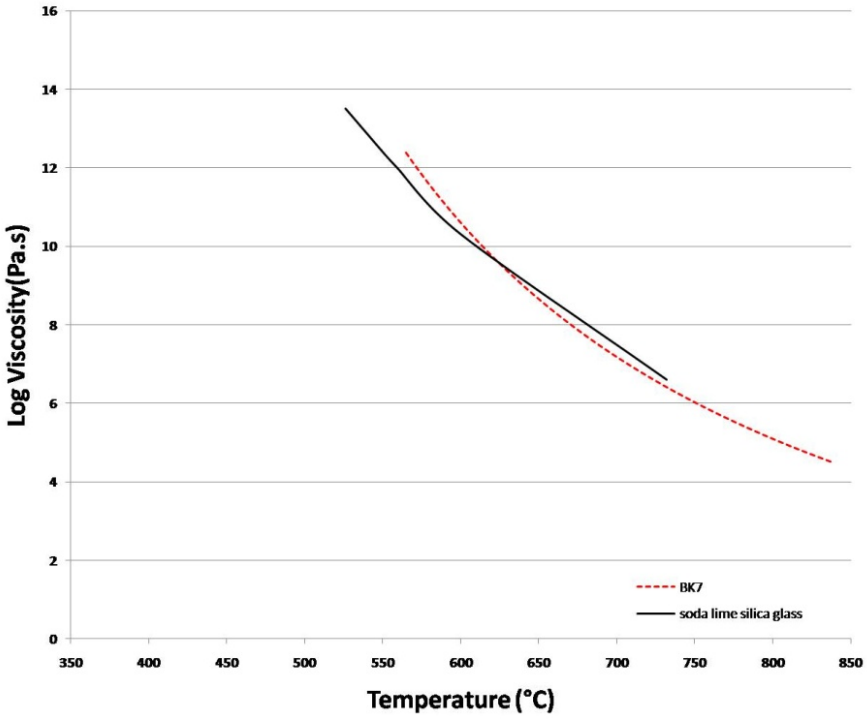

Figure 4-3: Viscosity versus temperature for BK7 and soda-lime-silica glass

4.1.2 Characterization of Glass Transition Temperature

In order to find the glass transition temperature of the glasses, Differential Scanning Calorimetry (DSC) measurements were performed using TA Instruments SDT 2960. The DSC measurements were taken in nitrogen atmosphere at a heating rate of 10°C per minute. The glass transition temperature (Tg) was determined from the DSC data curves and shown in Figure 4-4. Tg is 597°C and 593°C for BK-7 and soda-lime respectively based on the first inflection point of the endothermic peak. These data are in

a good agreement with the data reported by manufacturer and reported in Table 4-2 except that they are shifted. Again, the difference is the same as the difference reported by supplier but the whole data shifted by 40°C. This table also shows the thermal and physical properties of these glasses reported by supplier.

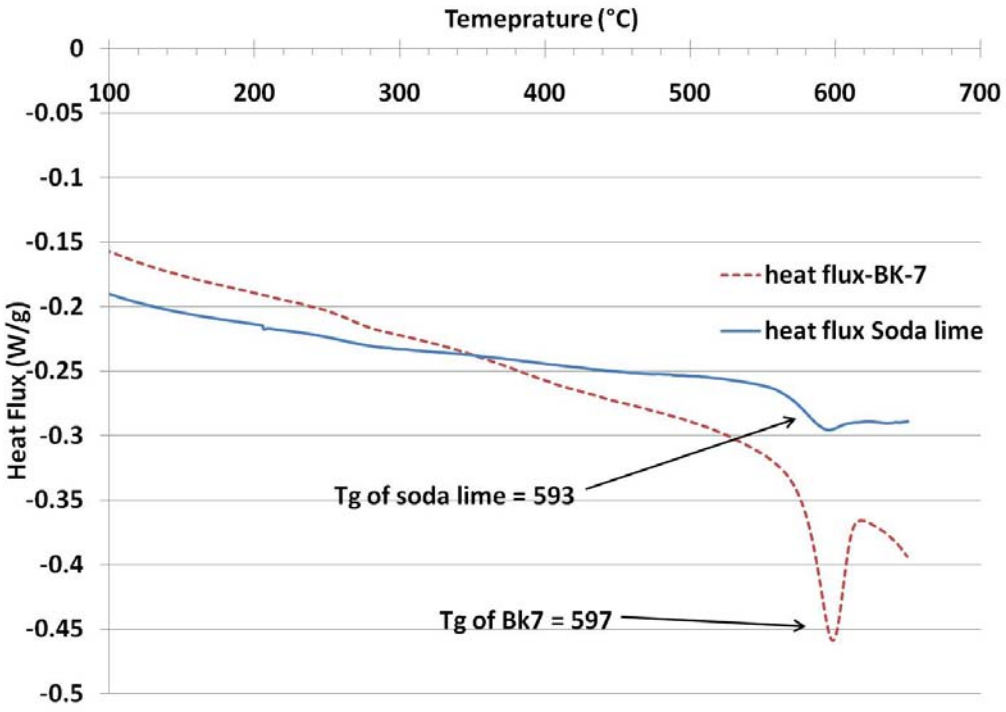

Figure 4-4: DSC curves for soda-lime and BK7 @ 10°C per minute

Table 4-2: Physical (at 20°C) and thermal properties of BK7 and Soda-lime reported by supplier

Glass type	Density (kg/m3)	Co. of thermal expansion (ppm)	Young's modulus (Gpa)	Poisson's Ratio	Thermal Conductivity (W/mK)	Tg by supplier (°C)
BK7	2510	7.1	82	0.206	1.114	557
Soda-lime	2500	9	73	0.23	1	552

4.1.3 Glass Viscoelasticity

Viscoelastic behavior is the time/frequency dependent response of a material to a strain or stress while elasticity is purely a stress-strain relationship. According to Findley *et al.* [23], this time dependent behavior must be expressed by a constitutive equation which includes time as a variable and relates stress and strain. In other words, the constitutive equation is representative of the stress history inside the material during the cycle time of loading and unloading in the forming process. This equation can be linear or non-linear based on the stress level. The material is said to be linearly viscoelastic if stress is proportional to strain at a given time and vice versa. As long as stress is low, the theory of linear viscoelasticity is valid for most oxide glasses according to Rekhson *et al.* [24], Duffrene [25], and Scherer [26].

The classic description and easy way to derive the viscoelastic constitutive equation is through the use of mechanical analogs. The simplest mechanical analog for a linear elastic material is a spring and for a pure viscous material it is a dashpot. A combination of these mechanical elements can be used to represent viscoelastic models. Maxwell and Voigt-Kelvin are the simplest models while three and four elements (Burger model) produce better models for actual materials [23].

In analytical modeling of materials, it is useful to separate shear strain and extensional strains mathematically. Shear strain is responsible for changing the shape of the body while extensional strain is responsible for both the shape and the volume of the body. In viscoelastic materials, the analytical model is separated to pure shear (deviatoric or shape change) and pure dilatation (spheric or volume change). In this study, there is an

interest in the deviatoric part of the response as the sliding between molds and glasses creates pure shear on glasses.

The Burger model is a good representative of pure shear. To understand the viscoelastic terminology used in this study, a creep-recovery analysis for a Burger model are briefly implemented as follows.

4.1.4 Theoretical Background of Creep (Response of System to Constant Stress)

The Burger model is a series combination of Maxwell and Kelvin models as shown in Figure 4-5.a. The constitutive equation for this model is:

$$\frac{\eta_1\eta_2}{G_1G_2}\ddot{\sigma}(t)+(\frac{\eta_1}{G_1}+\frac{\eta_1}{G_2}+\frac{\eta_2}{G_2})\dot{\sigma}(t)+\sigma(t)=\frac{\eta_1\eta_2}{G_2}\ddot{\varepsilon}(t)+\eta_1\dot{\varepsilon}(t) \qquad \text{Eqa. (4.2)}$$

where G and η are elastic shear modulus and viscosity of glass, respectively.

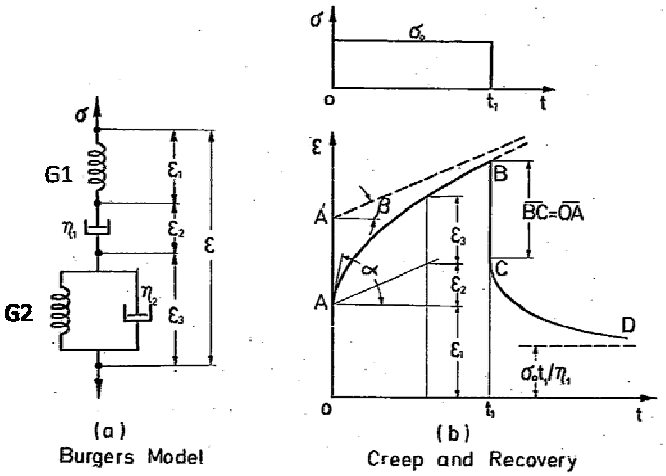

Figure 4-5: a) Mechanical analogue for Burger model b) Behavior of Burger model [23]

The strain response of this system under constant stress is the sum of the creep behavior of Maxwell and Kelvin models and is given by:

$$\varepsilon(t)=\frac{\sigma_0}{G_1}+\frac{\sigma_0}{\eta_1}t+\frac{\sigma_0}{G_2}(1-e^{-G_2t/\eta_2}) \qquad \text{Eqa. (4.3)}$$

The first two terms on the right hand side of Equation 4.3 represent instantaneous elastic strain and viscous flow while the last term represents the delayed-elasticity.

Differentiating Equation 4.3 yields the creep rate as:

$$\dot{\varepsilon}(t) = \frac{\sigma_0}{\eta_1} + \frac{\sigma_0}{\eta_2} e^{-G_2 t/\eta_2} \qquad \text{Eqa. (4.4)}$$

So, the creep rate at t=0+ has a finite value of $tg\alpha$ in Figure 4-5.b and can be calculated by:

$$\dot{\varepsilon}(0) = (\frac{1}{\eta_1} + \frac{1}{\eta_2})\sigma_0 = tg\alpha \qquad \text{Eqa. (4.5)}$$

And its value at infinity reaches $\frac{\sigma_0}{\eta_1}$ based on Equation 4.4. Figure 4-5 also shows that:

$$\dot{\varepsilon}(\infty) = \sigma_0 / \eta_1 = tg\beta$$

$$AA' = \sigma_0 / G_2 \qquad \text{Eqa.(4.6)}$$

$$OA = \sigma_0 / G_1$$

Thus, in theory the material constants of the Burger model can be determined by measuring the values of $\alpha, \beta, OA, and\ AA'$ in a creep experiment.

4.1.5 Theoretical Background of Stress Relaxation (Response of System to Constant Strain Rate)

The constitutive equation for a Burgers model can be also derived by considering the stress response under constant strain rate ($\varepsilon(t) = \varepsilon_0(t)$) as well. In this case, the constitutive equation has simplified to:

$$\frac{\eta_1\eta_2}{G_1G_2}\ddot{\sigma}(t) + (\frac{\eta_1}{G_1} + \frac{\eta_1}{G_2} + \frac{\eta_2}{G_2})\dot{\sigma}(t) + \sigma(t) = \eta_1\varepsilon_0 \qquad \text{Eqa. (4.7)}$$

where ε_0 is the slope of applied strain. The relaxation response can be found by applying the initial boundary condition of $\sigma(0) = \dot{\sigma}(0) = 0$. The solution to this linear ODE depends on the value of $\eta_1, \eta_2, G_1, G_2, and\ \varepsilon_0$. In MATLAB, the ode45 function can be used to numerically solve this linear second order differential equation.

For example, the response of the Burger model to $\varepsilon_0 = 0.1$ and considering $\eta_1 = 100\ Pa.s, \eta_2 = 10\ Pa.s, G_1 = 100\ GPa, G_2 = 5$ GPa is shown in Figure 4.6.

During friction testing, the apparatus imparts a constant shear strain rate to the glass. If the material is behaving viscoelastically, and there is no sliding, it can be expected that the force will vary in time in a manner similar to that shown in Figure 4-6.

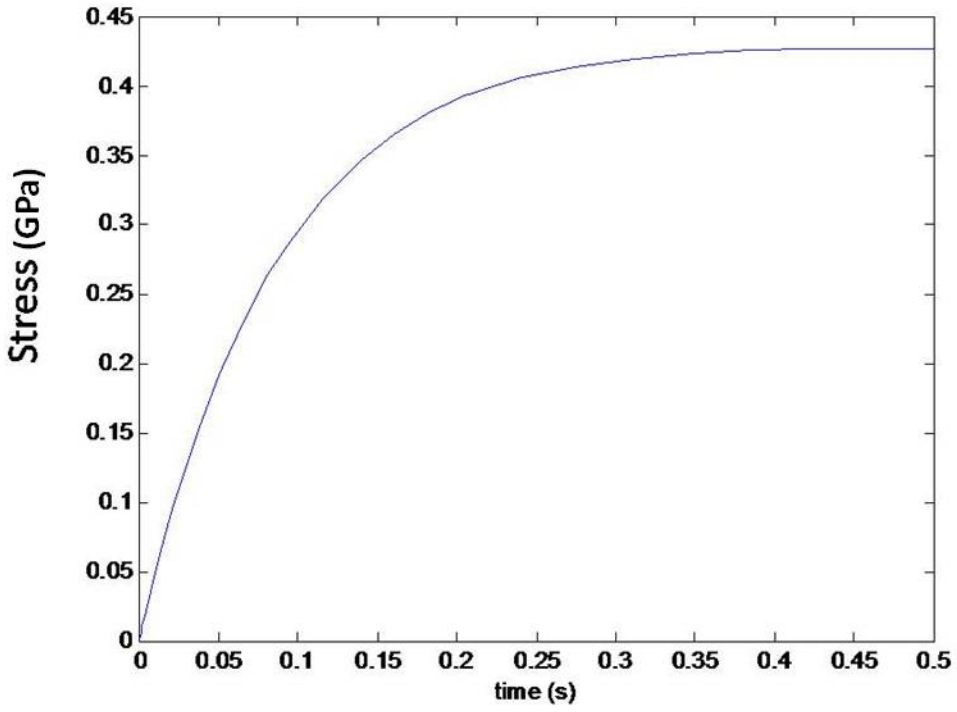

Figure 4-6: Stress relaxation response of Burger model to a constant strain rate

4.2 Mold Material

Tungsten Carbide (WC) was selected as a mold material as it has a high thermal conductivity, low thermal expansion, excellent wear resistance, excellent high temperature strength, and fine surface roughness which make it suitable for glass molding. The EMT 100NG grade (from Extramet Inc.) was used as a mold material for this study with physical properties listed in Table 4-3

Table 4-3: Tungsten Carbide properties

Tungsten Carbide	Grain Size (µm)	Density (g/cm^3)	Hardness HV 30	Transverse Rupture Strength (N/mm^2)	Coefficient of thermal expansion (ppm)	Thermal Conductivity (W/mK)
EMT100	< 0.8	14.85	1,717	> 3,900	4	41.87

4.3 Mold Coating

Without coating, the WC mold has a short lifetime because of chemical interaction between the mold surface and glass [27]. In this study, TiAlN-CrN-S4 commercially named as C2-SL + S4 (from Richter Precision Inc.) was used as a coating. It has a maximum working temperature of 950˚C which makes it suitable for our purpose.

4.4 Surface Roughness of Material

A Zygo scanning white light interferometer (New View 6K) was used to measure the mold and glass surface topography before each test to ensure that there was no residual glass stuck to the mold surfaces. Also, an optical microscope (Olympus SZX12) was used to qualitatively check the mold surfaces.

4.4.1 Mold Surface Condition

Two different surface conditions; ground, and polished (both coated) were used in this study. The roughness profiles of various areas for both conditions were observed and averaged to get the Root Mean Square (RMS) value of roughness as shown in Figure 4-7.a and 4-7.b. These figures show the RMS value of 672 and 38 nm for ground and polished molds, respectively. Also, Figure 4-7.a clearly shows the grinding marks left by the grinding wheel on the surface.

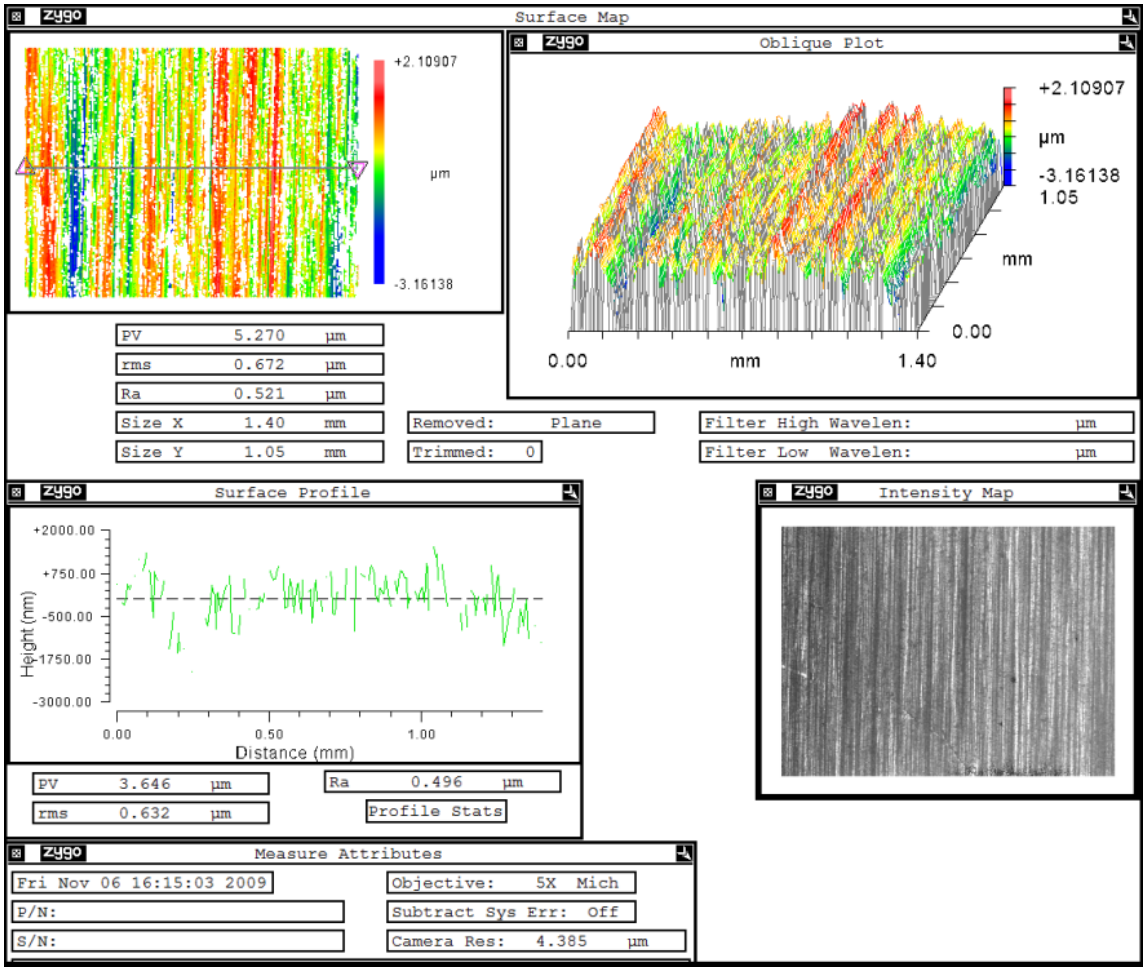

Figure 4-7.a: Surface roughness data for a ground and coated mold

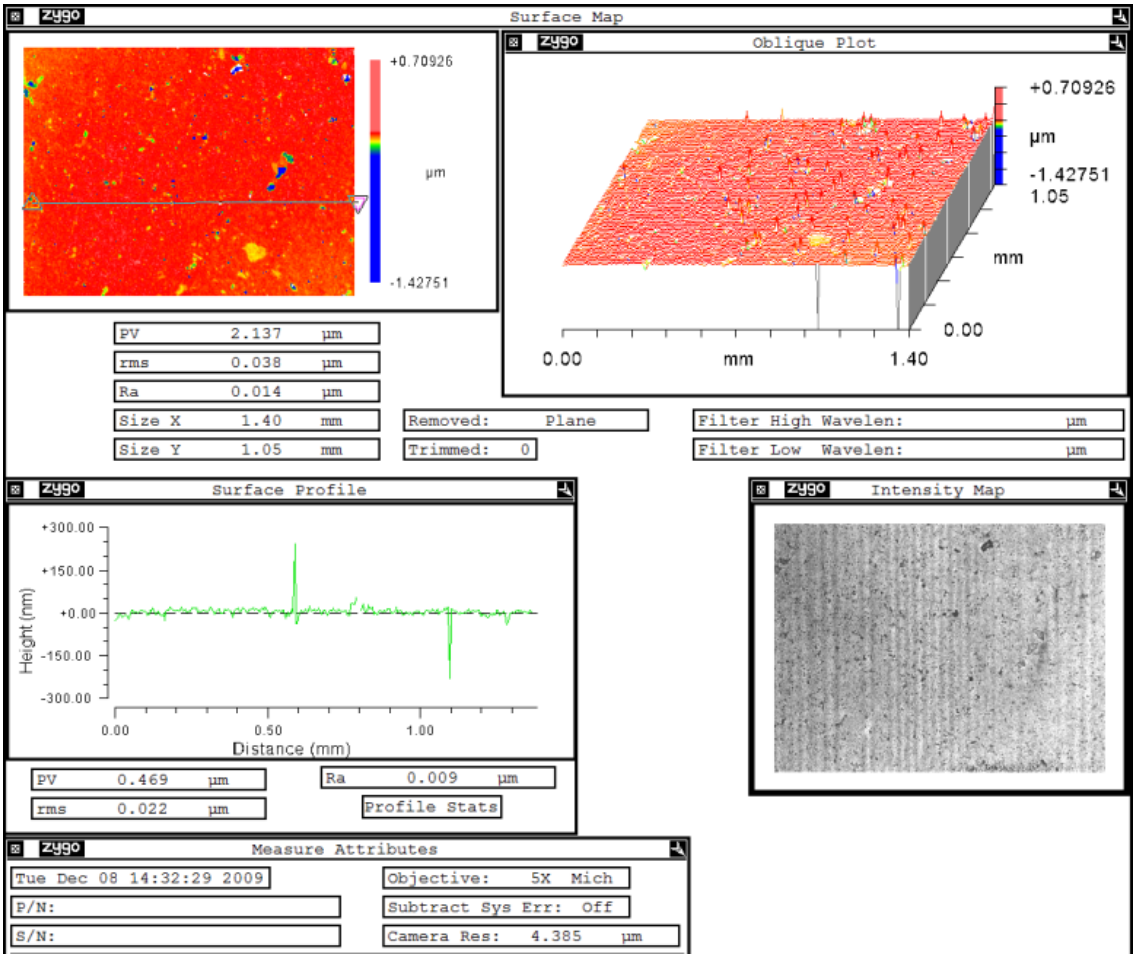

Figure 4-7.b: Surface roughness data for a polished and coated mold

The polishing procedure used in this study was selected based on Buehler's recommendation for refractory metals [28]. This is a four-step procedure to reach optical level surface roughness.

4.4.2 Glass Surface Condition

Both glasses used in this study had an RMS surface roughness value around 2 nm on the polished surfaces. For example, Figure 4-8 shows the surface roughness data for a BK7 sample after cleaning by inorganic solvents described in the next section.

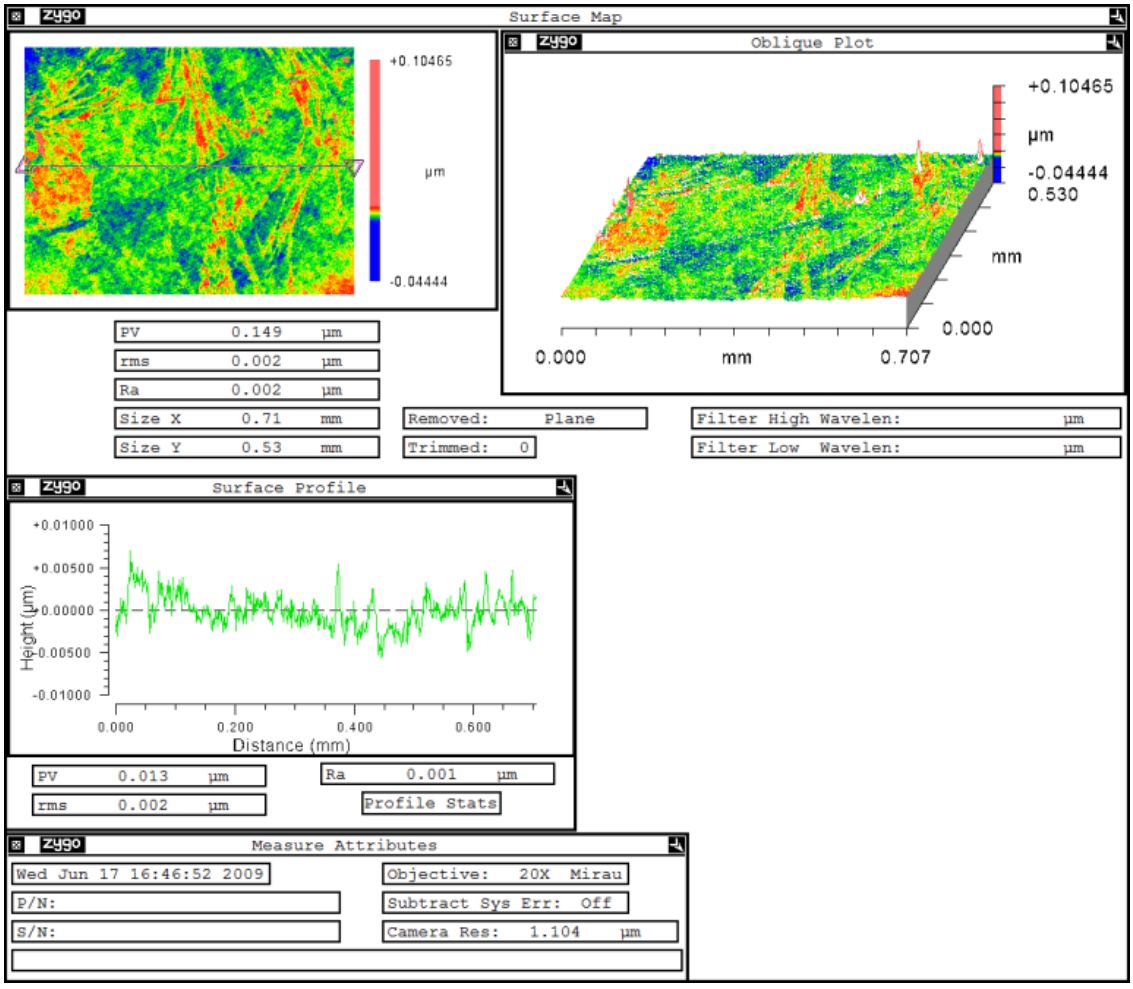

Figure 4-8: Surface roughness data for a cleaned BK7 glass

4.5 Cleaning Procedure

It is important to clean both surfaces before each trial, to prevent to damage to the coating or its interface with the substrate. Contaminants, whether on the mold or on the glass, can deteriorate the coating at high temperatures resulting in the sticking of glass to the mold material.

Unfortunately, the glass molding industry does not have established standards either for cleaning methods or even for the definition of what a “clean” optical surface is.

The only widely accepted method is the wipe technique using different types of solvent. In this method, a lint free tissue smoothly and continuously removes stains from surface. In this study three different solvents; acetone, ethanol, and isopropanol are used to clean the glass surface, respectively [Edmund Optics Inc.]. Also, after each molding trial, the mold surfaces needed to be thoroughly cleaned by acetone. The interferometric measurement of a piece of glass before and after cleaning has proven the effectiveness of cleaning by improving the surface finish on the order of 100 nm. As a result, this cleaning procedure was used for all trials in this research.

4.6 Oxidation

Oxidation is an intrinsic behavior of metal surfaces at high temperature. To prevent this phenomenon, oxygen should be removed from experimental environment and the cheapest way is by purging with high volumes of nitrogen.

4.6.1 Nitrogen Properties

Two grades of nitrogen (from Airgas Inc.) were used in this study; one high purity (HP) and the other ultra high purity (UHP). Different chemical components in these two grades are listed in Table 4-4. Both nitrogen grades have been used and prevented molds from oxidation.

Table 4-4: UHP and HP nitrogen different component

description	Grade	Min. Purity	Max. H2O (ppm)	Max. O2 (ppm)	Max. THC (ppm)	Max. Ar (ppm)	Max. CO2 (ppm)
UHP	5.0	99.999%	1	1	0.2	20	0.5
HP	4.8	99.998%	5	1	0.5	20	0.5

CHAPTER FIVE

EXPERIMENTAL RESULTS

5.1 Instantaneous and Average Friction Coefficient

There are two ways to quantitatively represent the friction coefficient in literature; one, instantaneous friction coefficient, and the other averaged friction coefficient. The former is used when there is no noise in the friction data and one can distinguish between static and dynamic friction clearly. In this case, the friction coefficient is calculated by dividing the frictional force by the normal force. Since friction is a nonlinear and discontinuous property as reported by Feeny *et al.* [29] and due to the normally distributed noise in the experimental data which is reported by Schmitz *et al.* [30], an average friction coefficient calculation was developed as following:

First, the friction work is calculated by:

$$W_i = \sum_{i=1}^{n} F_i * d_i, \ i = 1,2,3, \dots . n \qquad \text{Eqa. (5.1)}$$

Then, the average friction force at each point can be expressed as:

$$F_i = \frac{\sum_{i=1}^{n} F_i * d_i}{d_i}, \quad i = 1,2,3, \dots . n \qquad \text{Eqa. (5.2)}$$

Finally, the average friction coefficient can be calculated by dividing the average friction force to the normal force by:

$$\mu_i = \frac{F_i}{N_i} \qquad \text{Eqa. (5.3)}$$

where $\mu_i$is the average friction coefficient. By using this method, the average friction coefficient can be determined as a quantitative value.

5.2 Validation of Machine Functionality at Room Temperature for a Steel-Steel Friction Pair

Repeatability is the variability when the same person runs the same test repeatedly. To validate the basic functionality of the apparatus, repeatability tests were conducted at room temperature between a ground steel-steel friction pair, and the results compared to published data. For these tests, the normal force was adjusted to 100N and the feed rate to 1 mm/min. Both steel surfaces were ground with surface roughness of 435 μm (RMS value) and the room temperature was 22 ±1˚C. The results of sliding force (friction force), the data recorded by machine force transducer, versus displacement, data recorded by linear potentiometer installed on the bottom mold, are plotted in Figure 5-1. This figure clearly shows that the friction force increases to the onset of sliding at which time the dynamic friction becomes dominant. Both materials behave as an elastic solid and they slide against each other after reaching the limiting value of friction force at around 50 microns of total displacement.

Figure 5-2 shows the result of applying average friction coefficient calculation to the data of Figure 5-1. This figure shows that the friction coefficient increases until the sliding begins and then levels off with an essentially constant dynamic friction coefficient. The mean value of 0.17 achieved here as the dynamic friction coefficient value between a steel-steel pair at room temperature is in the range reported by Grigorier *el al.* [31] in their study, where they measured friction coefficient values of 0.15-0.2 for a steel-steel pair at room temperature.

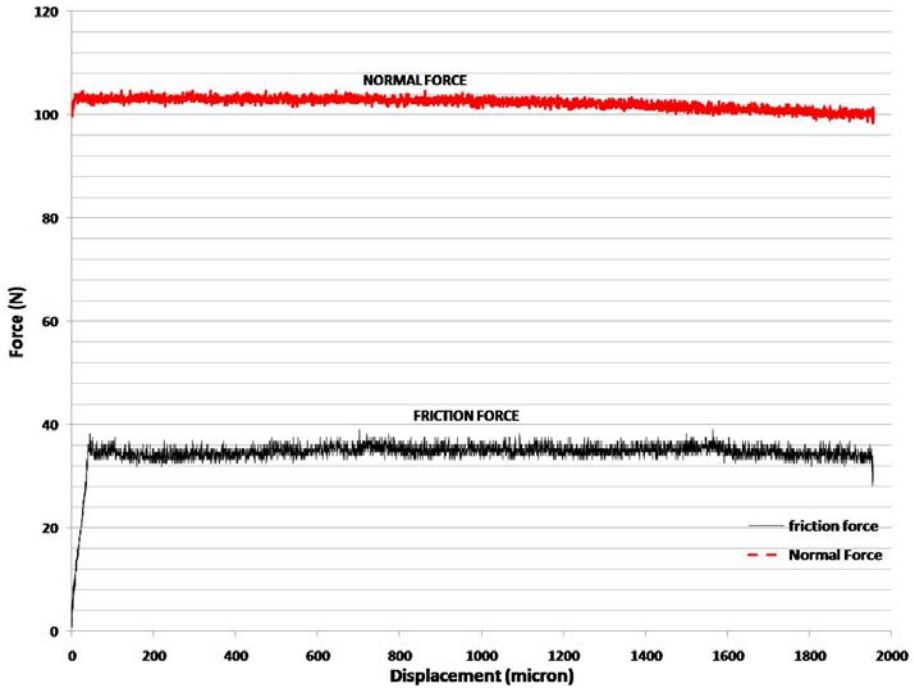

Figure 5-1: Frictional and normal force generated between a pair of steel- steel at room temperature

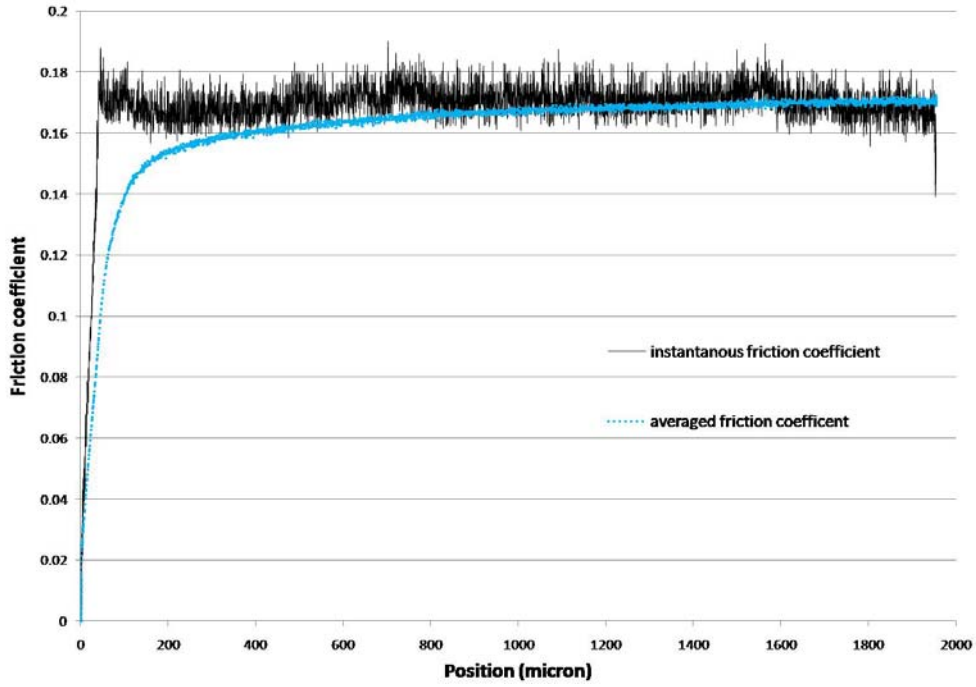

Figure 5-2: Friction coefficient curve between a pair of steel-steel at room temperature

5.3 Validation of Machine Functionality at Room Temperature for a Steel-BK7 Friction Pair

Again, another experiment with the same conditions as to the previous section was conducted using a steel-BK7 pair and the result of friction and normal forces versus displacement is shown in Figure 5-3. Also, instantaneous and average friction coefficients versus displacement are shown in Figure 5-4. This figure shows a lower value of friction coefficient for steel-BK7 pair since the glass has a lower surface finish in comparison to ground steel. Its friction coefficient is close to 0.1.

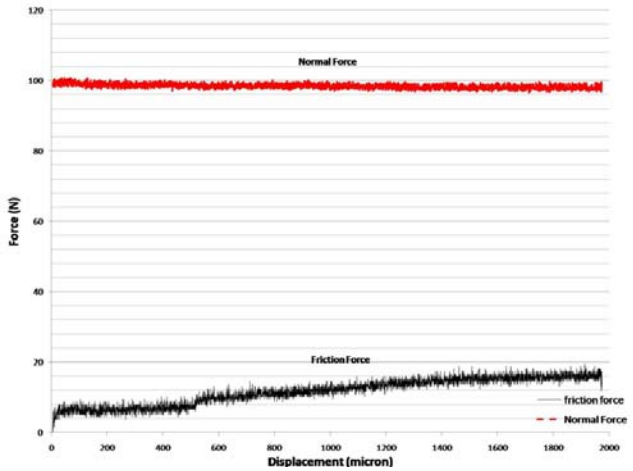

Figure 5-3: Frictional and normal force generated between a pair of steel-Bk7 at room temperature

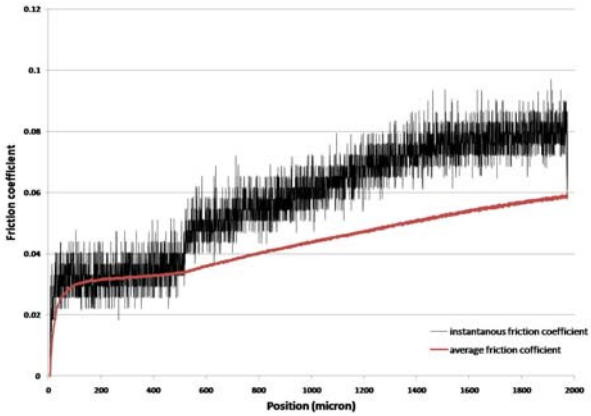

Figure 5-4: Friction coefficient curve between a pair of steel-BK7 at room temperature

5.4 Validation of Machine Functionality at High Temperature for a Pair of Steel-Steel & Steel-BK7 at Room Condition Environment (No nitrogen)

After validating the machine functionality, two trials; steel-steel and steel-BK7 glass pairs were conducted at elevated temperature. Again for these tests, the normal force was adjusted to 100N and the feed rate to 1 mm/min. The room temperature was 22 ±1˚C. The steel surfaces were polished with 320 grit size silicon carbide sandpaper while the BK7 had a surface finish of 2nm. Before testing, both surfaces of glass and mold were cleaned with acetone, ethanol, and isopropanol to be sure there was no contamination between the glass and the mold. The temperature and position vs. time profiles used for these tests are shown in Figure 5-5. A temperature of 577°C is used during these tests to ensure that the glass is above its glass transition temperature and behaves as a viscoelastic material.

First, the uncertainty of friction force and normal force due to the temperature is discussed and finally the results of friction coefficient for both pairs are presented later in this chapter.

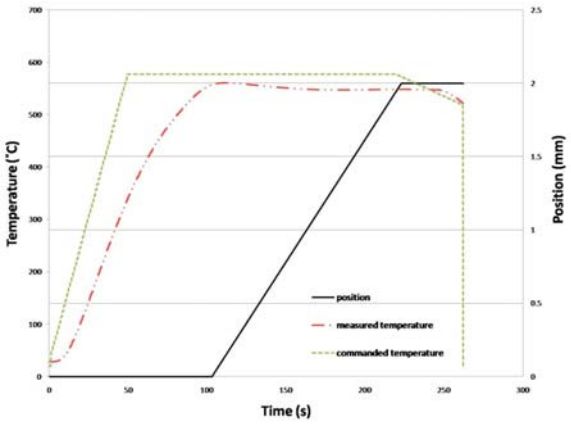

Figure 5-5: Temperature and position profile used for friction measurement between a pair of steel-steel and steel-BK7 at 577˚C

5.4.1 Uncertainty of Normal Force Due to the Temperature

The normal force may change due to thermal expansion between one end of the friction sample under test which is in contact with the hot mold and the other end which is in contact with the thermal break. The load cells used to monitor normal force are strain-gage based, and show significant sensitivity to change in temperature. Therefore, while they can be used to adjust the normal force during setup, they do not accurately monitor the force after heating of the system has begun. The variation in normal force can be estimated by considering thermal expansions of the elements in the load path.

The thermal break in our experiment is made of fine ceramic which has a low coefficient of thermal expansion. In the worst case, by assuming a thermal expansion coefficient of 10 ppm for all materials and assuming that the initial temperature is the room temperature, the maximum elongation in the normal load path is around 0.175 mm on each side.

Since there is a helical spring at the back of each force transducer as shown in Figure 5-6, this elongation may cause a change in the normal force. This force can be calculated from the stiffness of this spring, which is approximately 20 N/mm. So, the maximum force created by thermal expansion is on the order of 3.5 N, which is insignificant compared to the initial value of 100 N, meaning that the initial value of normal force can be used for the instantaneous friction coefficient calculation. Also, since the expansion of the movable and fixed members of the bottom mold tends to decrease the spring deflection, the worst case change in normal force is likely less than the above

described scenario. As a result, the normal force is considered to be the initial set value for instantaneous friction calculation.

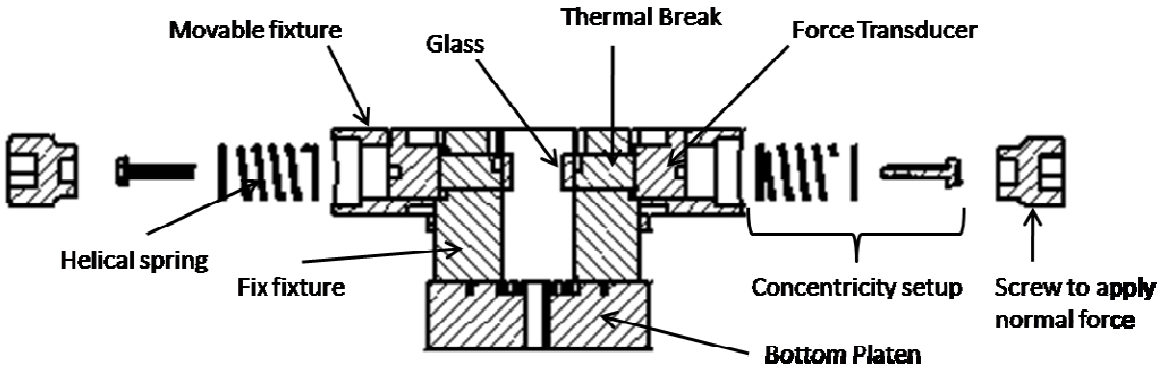

Figure 5-6: Section view of normal load path

5.4.2 Uncertainty of Friction Force Due to the Temperature

The temperature in the top mold is around 600°C for most of the experiments and consequently there is a large thermal expansion of the top mold. This elongation may result in a large force in the friction path if there is not free space for the top mold to expand. Since there is a hollow cylinder inside the fixed fixture in the bottom mold, the top mold can freely expand inside the bottom mold without creating any forces in the friction path. The only force created by this elongation is a shear force on the glass surface which is in contact with the mold. On the other hand, this elongation acts as a displacement with a constant strain rate on the glass, creating some shear force on glass. As a result, the thermal expansion created by temperature is recorded by the friction force transducer does not corrupt the friction force data.

Thermal drift could be another source of error on friction force measurement if the temperature of the strain gage force transducer differs from the original set point temperature, which in this case is room temperature. To find the thermal drift of the force

transducer, a test using a WC-BK7 pair at high temperature (600 °C) and long time (1250 sec) was conducted. In this test, the commanded position was held constant, and the resulting plot of measured "friction" force versus time is illustrated in Figure 5-7.

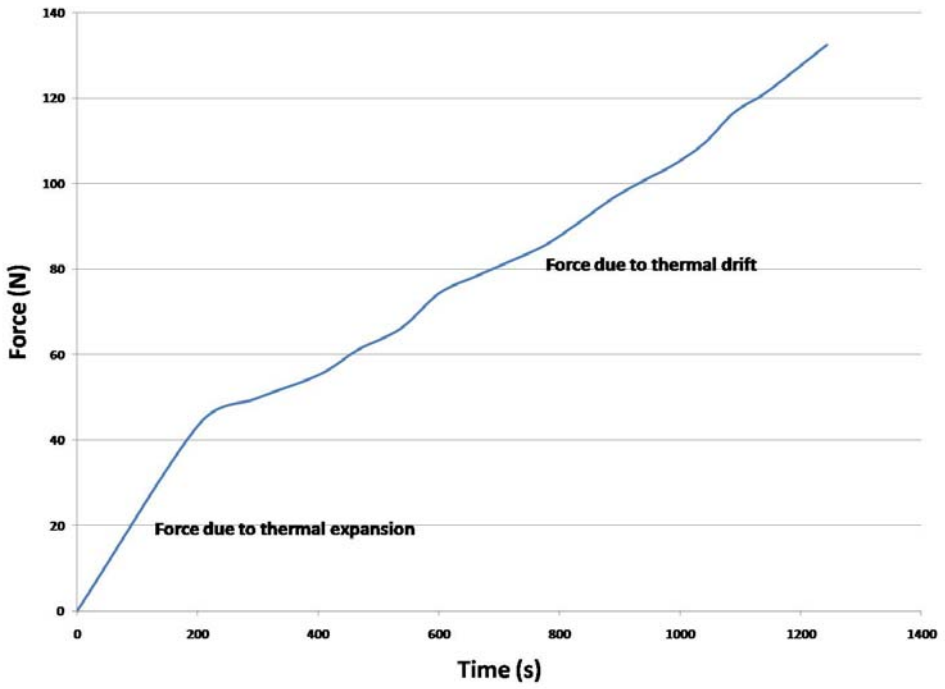

Figure 5-7: The effect of thermal drift on friction force

Since the position is constant, the build-up of the measured force is due to thermal expansion of the WC mold carrier and the thermal drift of the force transducer. The temperature of the WC mold carrier reaches equilibrium fairly quickly, at about 200 seconds in the plot above. The temperature of the force transducer takes much longer to develop due to the ceramic thermal break between the mold carrier and the load cell. Figure 5-7 shows that the measured force increases approximately linearly with time at a rate of 0.085 N/sec. All subsequent friction force data reported in this dissertation will have this time dependent behavior of the load cell deducted from the raw data.

5.4.3 The Friction Data for a Steel-Steel and Steel-BK7 Pairs at Elevated Temperature

Finally, the result of friction force versus displacement for a pair of steel-steel and a pair of steel-BK7 is shown in Figure 5-8 and Figure 5-9, respectively. These figures show substantially more complex friction behavior than for the room temperature steel-steel pair. Both figures clearly show an increase in friction force with increasing temperature which is also reported by Rangnatha *et al.* [32].

As Figure 5-8 shows, for the high temperature steel-steel pair, sliding behavior is reached early after backlash between the normal (horizontal) and frictional force (vertical) path is removed. From that time the friction force stays constant until about 1200 microns of displacement and then due to some anomaly encountered in the surface, or perhaps even galling that can occur with self-mated materials, it rises. In Figure 5-9, for the high temperature steel-BK7 pair the friction force increases based on the viscoelastic response of material to constant strain rate as discussed in Section 4.1.5. The Burger model explains clearly that the stress relaxation response of a viscoelastic material to a constant strain rate has similar trend to that shown in Figure 4-5, and explains why the friction force is rising over time.

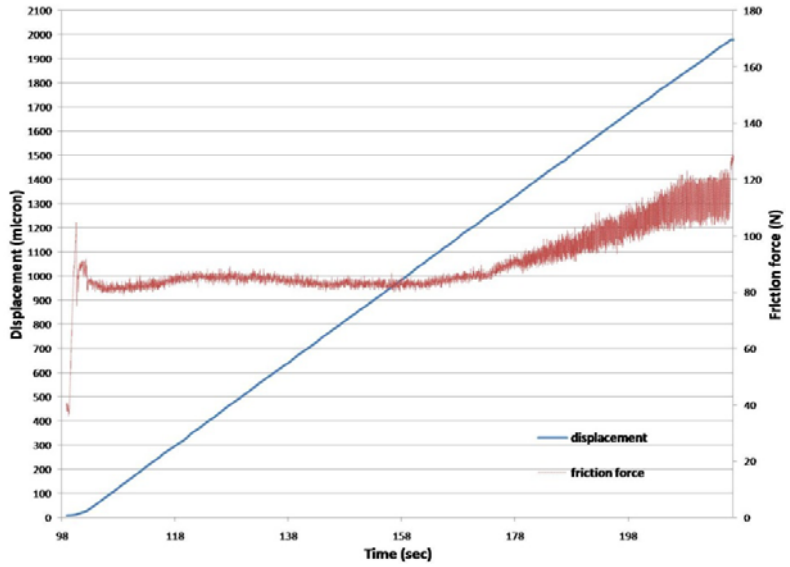

Figure 5-8: Frictional force generated between a pair of steel- steel at 577˚C

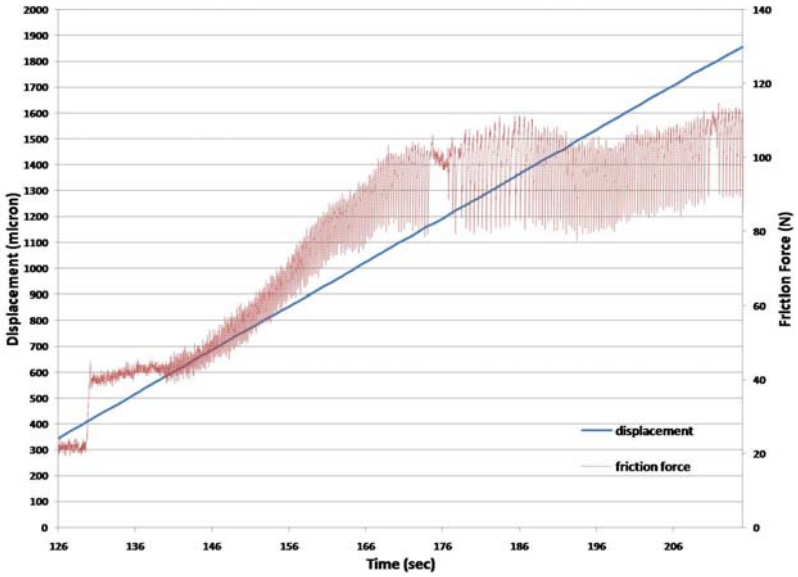

Figure 5-9: Frictional force generated between a pair of steel-BK7 at 577˚C

Moreover, both figures include regions of stick-slip phenomenon clearly visible when the position reaches around 1200 microns. Figure 5-10 and Figure 5-11 provide a zoomed-in view of this portion of the graphs showing two different types of stick-slip

phenomena. The first one is between two elastic bodies (steel-steel) and the other between an elastic and viscoelastic body (steel-BK7). This stick-slip phenomena is still in good agreement with the results reported by Persson [33] except that the second one shows the apparent effect of viscoelastic behavior of glass on the response, meaning viscoelasticity changes the stick behavior response in dynamic friction measurement.

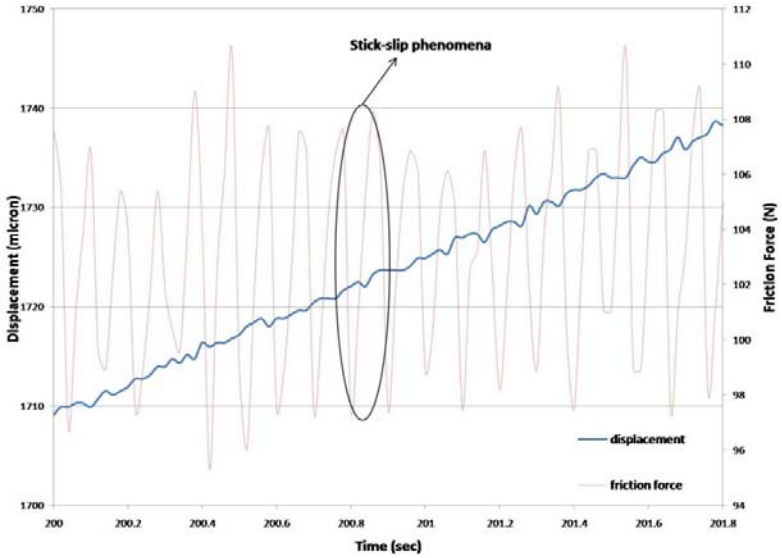

Figure 5-10: Stick-slip phenomenon between a pair of steel-steel at 577˚C (zoomed-in view of Figure 5-8)

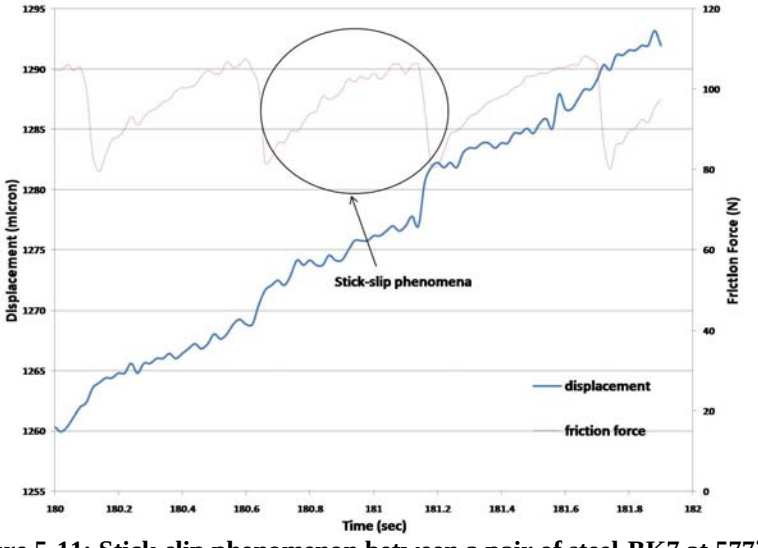

Figure 5-11: Stick-slip phenomenon between a pair of steel-BK7 at 577˚C (zoomed-in view of Figure 5-9)

5.4.4 Friction Coefficient at High Temperature for a Pair of Steel-Steel and Steel-BK7

The kinematic friction coefficient cannot be directly deduced when there is stick-slip oscillation in friction data. Instead, the instantaneous friction coefficient can be used. The instantaneous friction coefficients for both of these tests are plotted in Figure 5-12 and Figure 5-13, respectively. Both figures again show the stick-slip phenomena on the friction coefficient.

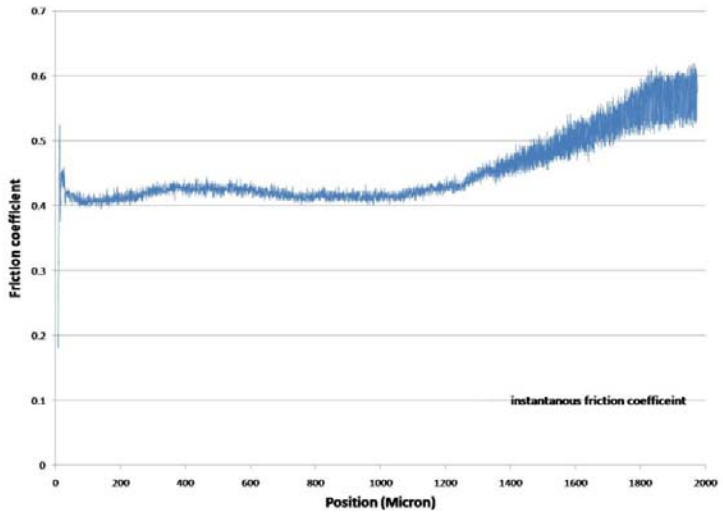

Figure 5-12: Instantaneous friction coefficient curve between a pair of steel-steel at 577˚C

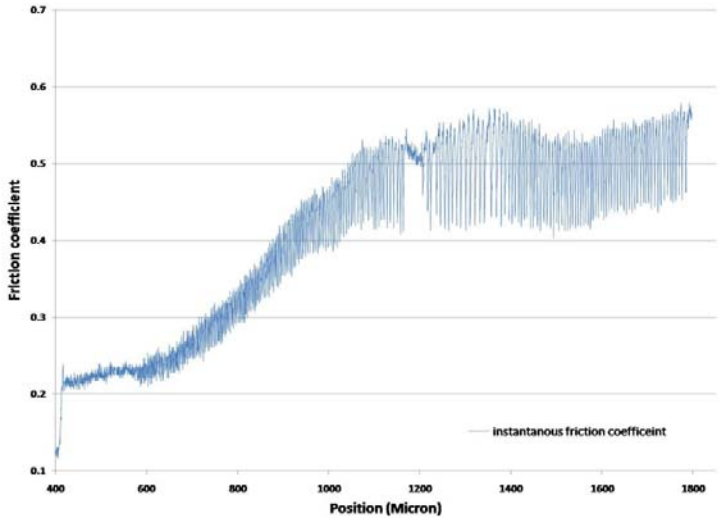

Figure 5-13: Instantaneous friction coefficient curve between a pair of steel-BK7 at 577˚C

5.5 The Important Parameters Affecting Friction Curves for Glass Molding

5.5.1 Temperature

In friction measurements for glass molding, temperature has a significant role because it changes the viscosity of glass drastically. For example for BK7, changing the temperature from 565˚C to 588˚C changes the viscosity from $10^{12.38}$ Pa.s to $10^{11.15}$ Pa.s, meaning that raising the temperature by 20˚C changes the viscosity by one order of magnitude.

In order to find the effect of temperature on friction data, a group of tests using a steel-BK7 pair have been conducted at different temperatures and the results are plotted in Figure 5-14. For these tests, all the other process parameters are held constant at the same values described in Section 5.4. This figure shows that the friction force begins to rise after the temperature reaches approximately 325˚C, similar to what happens between steel-steel at high temperature. Still, at temperatures well below Tg, such as 400˚C, BK7 behaves as an elastic material and there is no significant viscoelastic response of the material to applied load as shown in Figure 5-15. Raising the temperature close to the glass transition temperature of glass causes the viscoelastic response of material in the stick-slip regime of frictional force as shown in Figure 5-11.

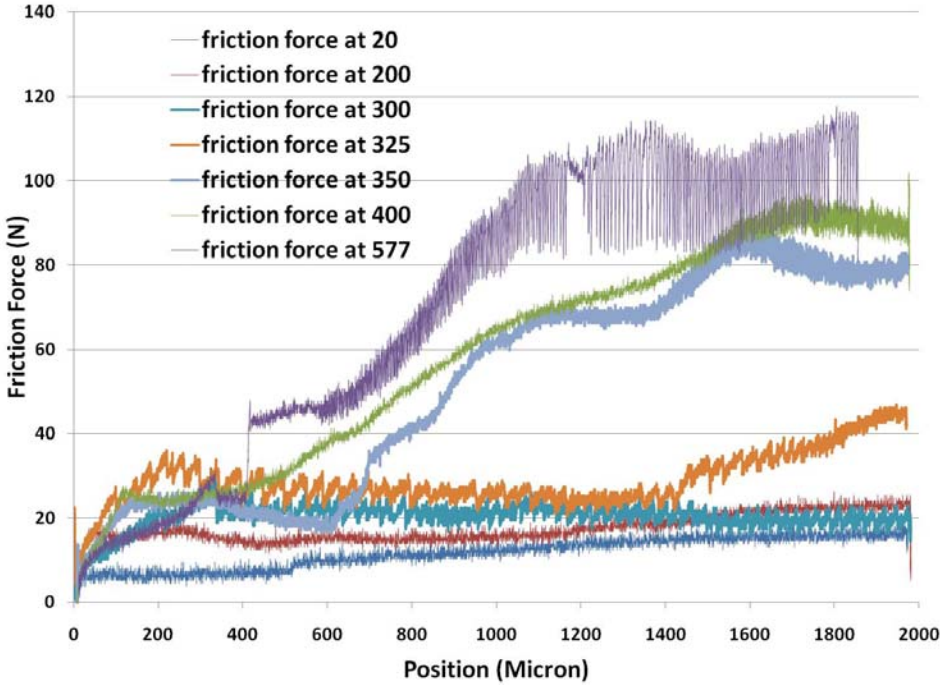

Figure 5-14: Frictional force curve between a pair of steel-BK7 at different temperature (feed rates 1 mm/min, Normal force 100 N, and no externally applied UHP nitrogen)

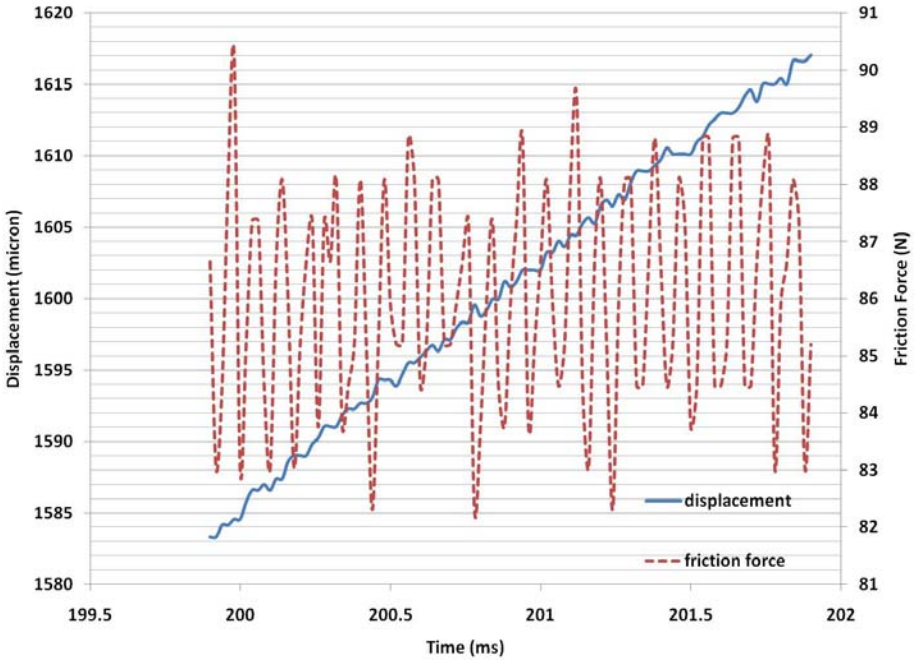

Figure 5-15: Stick-slip phenomenon between a pair of steel-BK7 at 400˚C (zoomed-in view of Figure 5-14)

5.5.2 Feed rate

For proper measurement of friction, it is necessary to minimize the thermal and elastic structural loop of apparatus. Research conducted by B. N. J. Persson [33] and A. D. Berman [34] using the surface force apparatus shows the effect of stiffness, velocity and mass on friction data. They show different regimes from stick-slip to steady sliding in their study depending on the structural loop mass and stiffness and the sliding velocity.

The machine used in this research is designed for very high PGM forces (up to 20,000 N) and temperatures up to 800˚C. Also, it has a closed structural loop which makes it suitable for measuring stick-slip phenomena. However, the structural dynamics of the machine can affect the friction data as the vertical axis of the machine (friction force path) has finite stiffness and mass. Depending on the feed rate or nominal sliding speed of the test, the dynamic structural response of the machine may affect the friction data. To investigate this effect, two trials one at high feed rate (10 mm/min) and the other at low feed rate (1 mm/min) using a steel-BK7 pair were conducted at room temperature and the results are plotted in Figure 5-16. Again, the other process parameters are similar to Section 5.4. These plots clearly explain the effect of feed rate on the friction force. As a result, feed rate affects the friction coefficient at high temperature as well and needs to be considered.

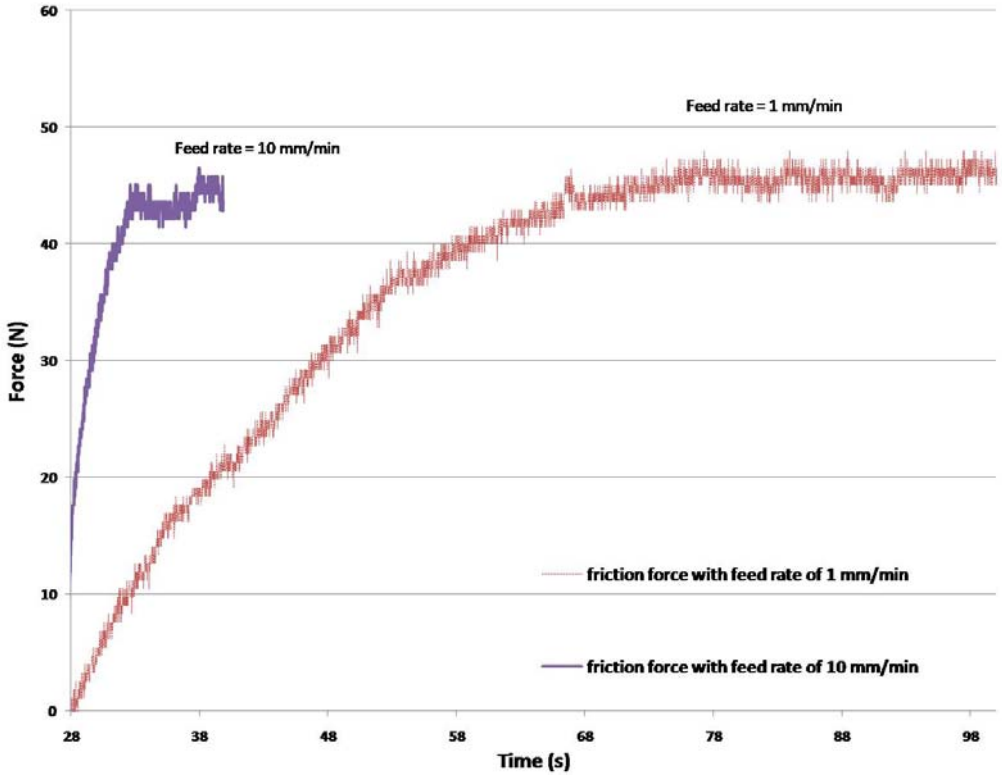

Figure 5-16: The effect of feed rate on friction force for a pair of steel-BK7 at room temperature

5.5.3 Normal Load

To investigate the effect the of normal load on friction data, a trial using a polished and coated WC mold-soda lime silica glass pair was used when the normal force was adjusted to 120 N and the result is presented in Figure 5-17. Again, the feed rate was 1 mm/min, and the test was conducted at room temperature. An instantaneous friction coefficient of 0.1 was observed. This value is in good agreement with the results of measurement in Section 5.3 and it shows that variations in the normal force don't affect the friction coefficient. The Coulomb's model which is the ratio of friction force to normal force should be a constant value for a pair of known material regardless of the applied load. Consequently, increasing the normal force increases the friction force proportionally for materials with constant friction coefficient.

But at high temperatures, increasing the normal load decreases the gap between hot mold and glass and consequently the gap conductivity increases, meaning that there will be a better thermal path between mold and glass. Having a higher temperature at the interface affects the viscosity behavior of glass and consequently the friction coefficient changes. So, the normal load at high temperature may affect the friction and need to be considered.

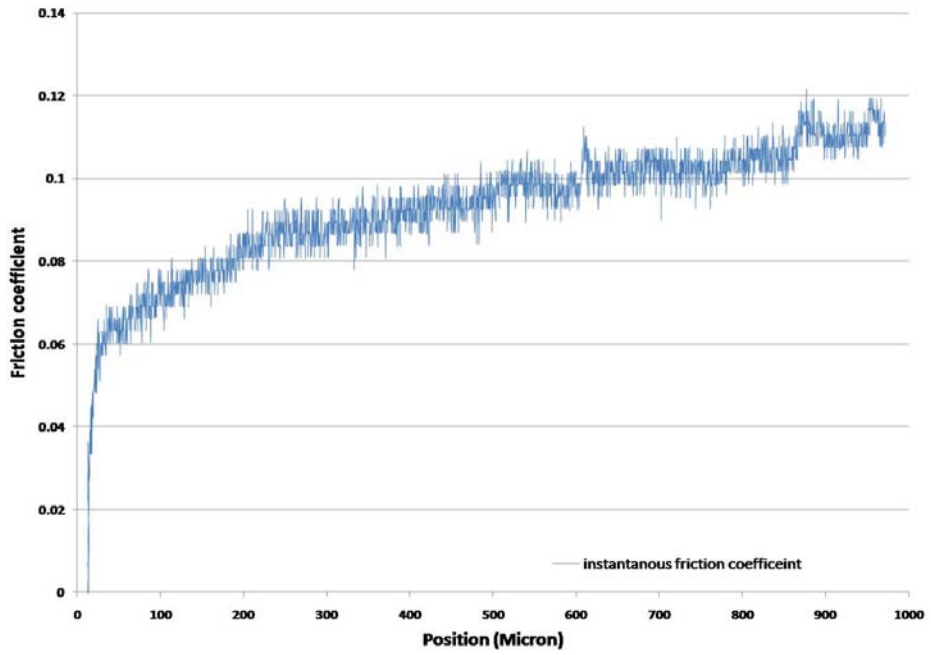

Figure 5-17: Instantaneous friction coefficient between a pair of polished and coated WC-soda lime glass at room temperature and normal load of 120 N

5.5.4 Surface Roughness

Surface roughness is a critical factor (at room temperature) as reported in most friction data handbooks. To investigate the effect of surface roughness on friction coefficient, a test using a pair of steel-steel with mold surface roughness (RMS) value of 3.136 µm was conducted at room temperature and the result is shown in Figure 5-18.

Again, the other process parameters are similar to Section 5.2. As this figure shows, the average friction coefficient of 0.28 was observed.

Comparing the friction coefficient values confirms the effect of surface roughness on friction data at room temperature. So, it can be an important factor at high temperature as well.

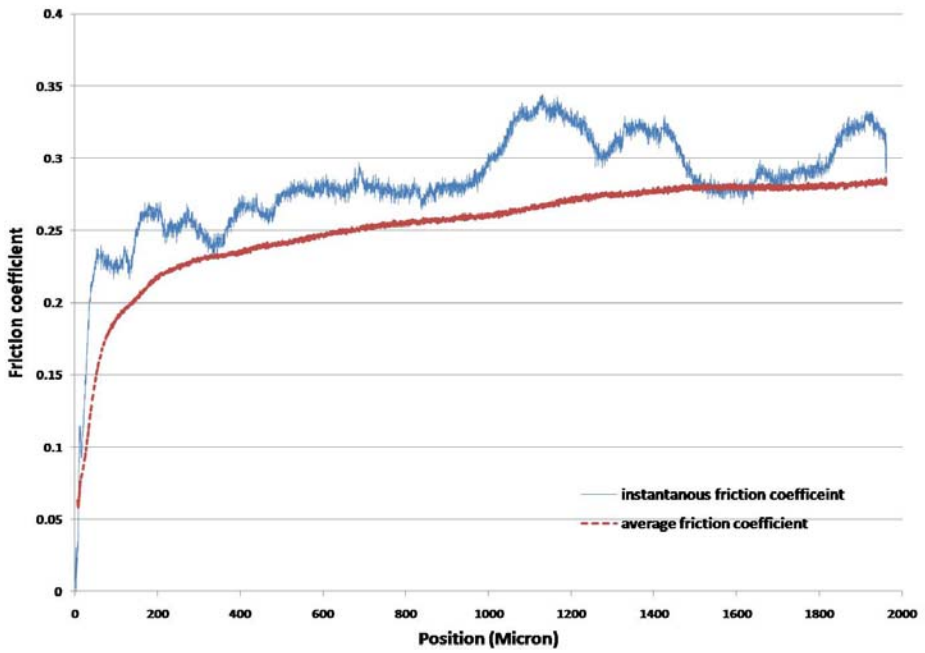

Figure 5-18: Friction coefficient curve between a pair of steel-steel with high surface roughness at room temperature

5.5.5 Glass Type

The glass behavior close to glass transition temperature depends on the thermal history of glass during manufacturing. The cooling rate of a super-cooled liquid can affect the fictive temperature, which is the artificial quantitative representation of deviation from equilibrium, and consequently the properties of that particular glass can alter.

Here, another series of experiments were conducted using steel-soda lime silica glass pair with conditions similar to ones mentioned in Section 5.5.1 and the results are shown in Figure 5-19.

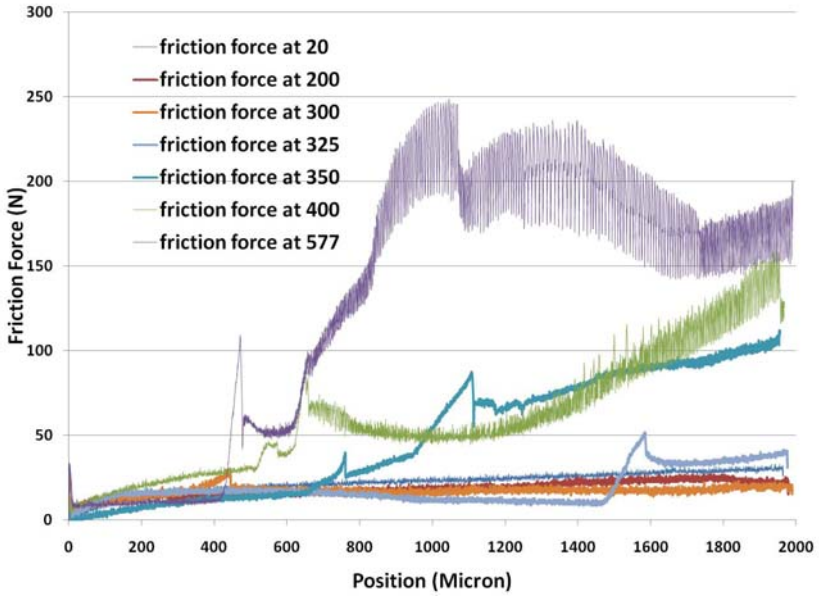

Figure 5-19: Frictional force curve between a pair of steel-soda lime silica glass at different temperature (feed rates 1 mm/min, Normal force 100 N, and no externally applied UHP nitrogen)

Again, this figure shows that the friction behavior begins to rise after the temperature reaches to 325˚C similar to what happens between steel-BK7 at high temperature. Still, at temperatures well below Tg, such as 400˚C, soda lime behaves as an elastic material in stick-slip regime of frictional force and there is no significant viscoelastic response of material to applied load as shown in Figure 5-20. Raising the temperature close to glass transition temperature of glass causes the viscoelastic response of material in the stick-slip regime of frictional force as shown in Figure 5-21.

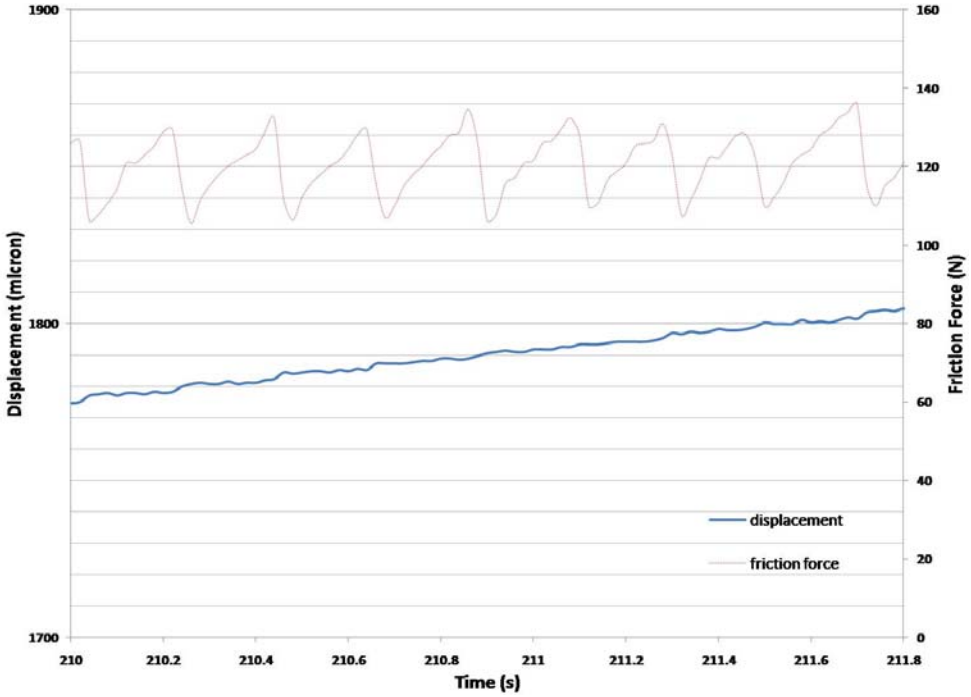

Figure 5-20: Stick-slip phenomenon between a pair of steel-soda lime at 400˚C (zoomed-in view of Figure 5-19)

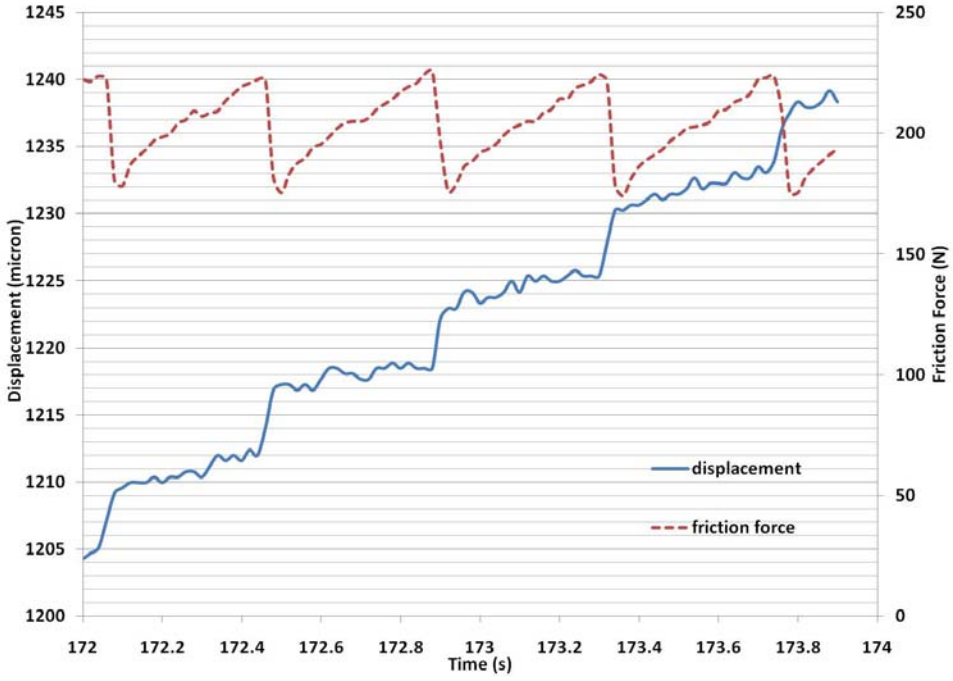

Figure 5-21: Stick-slip phenomenon between a pair of steel-soda lime at 577˚C (zoomed-in view of Figure 5-19)

The only difference between the two friction force data (compare Figure 5-19 and Figure 5-14) is the friction force amplitude. So, it can be seen that the use of different glass types results in different values of friction coefficient.

5.6 The Friction Force between Polished and Coated WC-BK7 Pair at Conditions Similar to Glass Molding Process

A set of tests at different elevated temperature using polished and coated WC-BK7 pair were conducted and the results are shown in Figure 5-22. These curves clearly show that the friction force is increasing with increasing temperature. This may be related to the viscoelastic behavior of BK7 at elevated temperatures. Friction is related to the mechanical interlock between two bodies and glass properties vary substantially with temperature, as described in reference [1]; the friction force is strongly dependent on temperature.

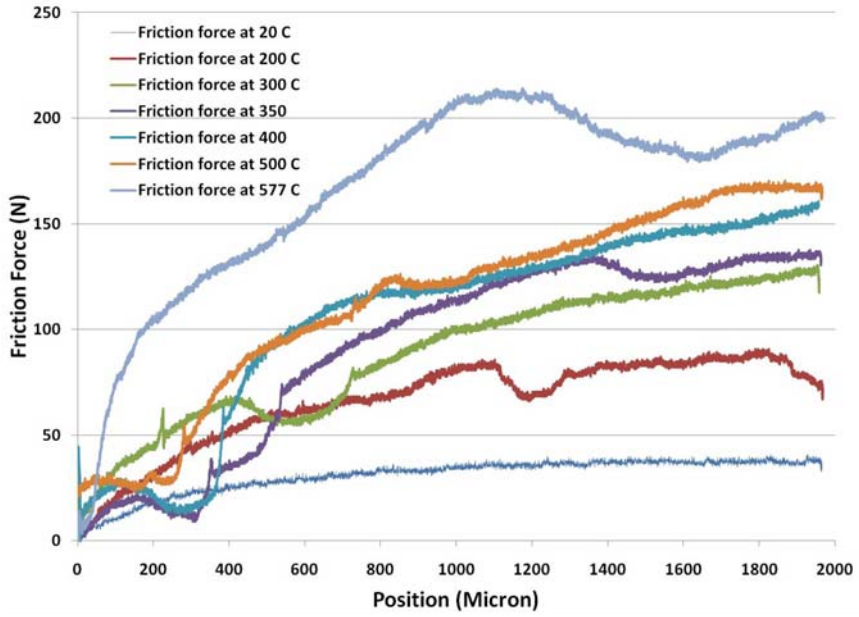

Figure 5-22: Friction force generated between a pair of polished and coated WC-BK7 at 20, 200, 300, 350, 400, 500, and 577˚C

Also, at temperatures close to the glass transition temperature, Tg, which is 557˚C for BK7, the glass exhibits a viscoelastic response to applied loads while WC is in the elastic regime. This glass viscoelasticity introduces time dependent response to the dynamic friction data; meaning that the feed rate of the test can affect the measured frictional load.

Stick-slip was not observed on any of these tests since the molds used have high surface finish and are coated to prevent chemical interaction between the glass and mold surface, and are conducted in an atmosphere of UHP nitrogen.

To evaluate the repeatability of the friction test at temperatures close to Tg, multiple tests for coated and polished WC-BK7 pairs were conducted at 560˚C and the results are shown in Figure 5-23. The repeatability results show that the change in friction force is less than 30 N which is 20% of maximum friction force.

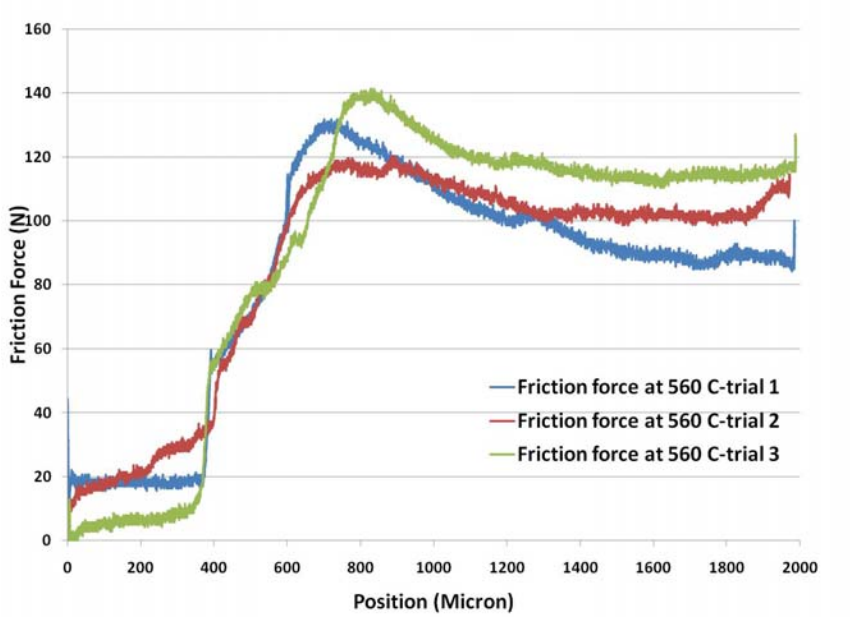

Figure 5-23: Friction force generated between a pair of polished and coated WC-BK7 at 560˚C for three trials with same process parameters at the same conditions

Dividing the friction force by the normal force, which is 100 N on each side, gives the instantaneous normalized friction coefficient data. These data are plotted in Figure 5-24 and they show that in the worst-case scenario, the normalized friction coefficient ramps up to 0.7 and then levels off at around 0.6. There is a smooth transition between static and dynamic friction.

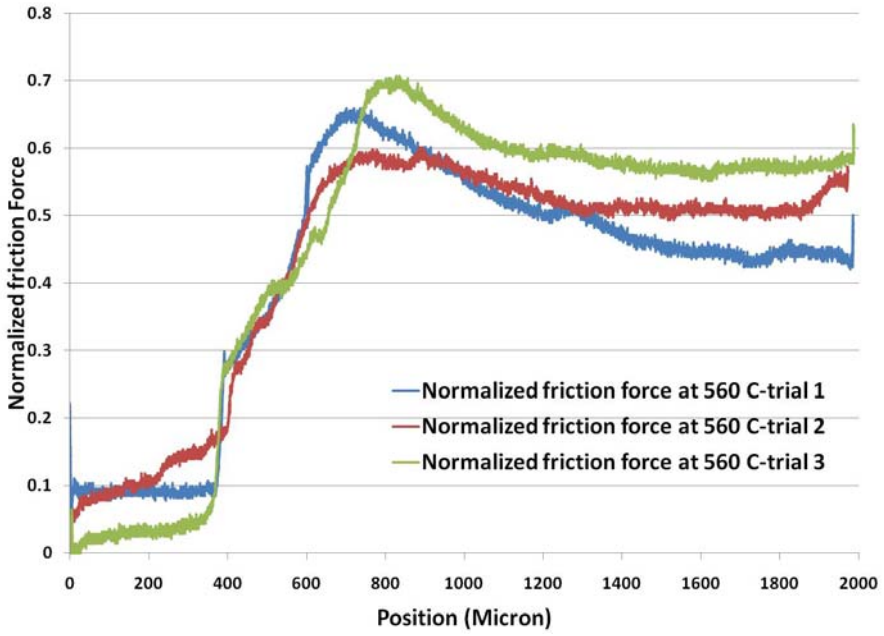

Figure 5-24: Friction coefficient from Figure 5-23

5.7 Design of Experiment

Since multiple parameters may affect the measured friction coefficient, the Design of Experiment (DOE) technique is implemented to study the effect of these parameters systematically. DOE refers to an experimental framework used to quantify indeterminate measurements of factors and interactions between factors statistically through observance of forced changes made methodically as directed by mathematically

systematic tables. The DOE technique is based on making deliberate changes to one or more factors in order to observe the effect these changes have on the response.

It is applicable in various scenarios such as achieving a desired target for the process which is similar to fine tuning a process, maximizing or minimizing a response or to find the key factors leading to a particular response, or to make the given process robust. In this study the aim is to find the key factors affecting the friction coefficient. Its primary purpose here is to identify significant main effects, rather than interaction effects. Some of the common terms used when dealing with this type of DOE are:

- Factors are the parameters that can be controlled and influence the performance of the final result.
- Levels of a parameter are the values that can show the parameter variability in its range; low, intermediate, and high levels.
- Response of the DOE is the performance or the output achieved for the particular combination of factors at particular level.

Since there is a mixed combination of levels and the goal is to find the main effects of parameters on friction with a relatively few number of experiments, the orthogonal array (Taguchi) method is a suitable approach to select the test parameters. An important advantage of using this method is that the experimental matrix is orthogonal in nature [35]. Orthogonality ensures that the estimate of any particular factor on the response will not be distorted by the effects of other factors; meaning that the effect of each factor can be mathematically calculated independent of the other factors. In this method, the experimental matrix is defined by the number of parameters and their levels.

In this research, there are five main process parameters, each of them at different levels as listed below:

1-Glass material at two levels; BK7 and soda-lime-silica glass

2- Normal load (N) at two levels; 100, 120

3- Feed rate or the relative velocity (mm/min) at two levels; 0.1, 1

4- Temperature at two levels; (Tg+20) 577˚C and (Tg+50) 600˚C

5- Mold surface condition at two levels; ground coated, and polished coated

A standard L8 Taguchi array matrix along with the actual values for the process parameters is selected and shown in Table 5-1 and Table 5-2, respectively.

Table 5-1: Standard L8 Taguchi array matrix

Run	X1	X2	X3	X4	X5
1	1	1	1	1	1
2	1	1	1	2	2
3	1	2	2	1	1
4	1	2	2	2	2
5	2	1	2	1	2
6	2	1	2	2	1
7	2	2	1	1	2
8	2	2	1	2	1

Table 5-2: Actual value for experimental matrix based on Table 5-1

Experiment	Glass Material	Normal load (N)	Feed Rate(mm/min)	Temperature (˚C)	Surface Condition
1	Soda lime	100	0.1	Tg+20	Ground coated
2	Soda lime	100	0.1	Tg+50	Polished coated
3	Soda lime	120	1	Tg+20	Ground coated
4	Soda lime	120	1	Tg+50	Polished coated
5	Bk7	100	1	Tg+20	Polished coated
6	Bk7	100	1	Tg+50	Ground coated
7	Bk7	120	0.1	Tg+20	Polished coated
8	Bk7	120	0.1	Tg+50	Ground coated

Once the experimental design was finalized, the friction tests were carried out in the absence of a clean room environment to assess how robust and feasible the process is. The trial was carried out from the same piece of the molding material (WC) at different surface conditions; ground, and polished. After each molding trial, the mold surfaces were thoroughly cleaned by acetone. Also, the glass samples were cleaned using lint-free optical wipes and reagent-grade acetone, ethanol, and isopropanol, respectively. These solvents were used in order to dissolve any organic and inorganic contaminations that might be adhering on the glass surface. Moreover, all eight experiments were conducted using UHP nitrogen. Finally, the collected data is analyzed and the results obtained are used to interpret the friction phenomenon of precision glass molding in next chapter.

As the experimental matrix shows, there are four combinations of feed rate and temperature values which results in four different temperature and position profiles for the tests. Each of these profiles is illustrated in Figures 5-25, 5-26, 5-27, and 5-28. Also, the friction coefficient versus position curves for experiments number 1, 2, 3, 4, 5, 6, 7, and 8 are shown in Figures 5-29, 5-30, 5-31, 5-32, 5-33, 5-34, 5-35, and 5-36, respectively.

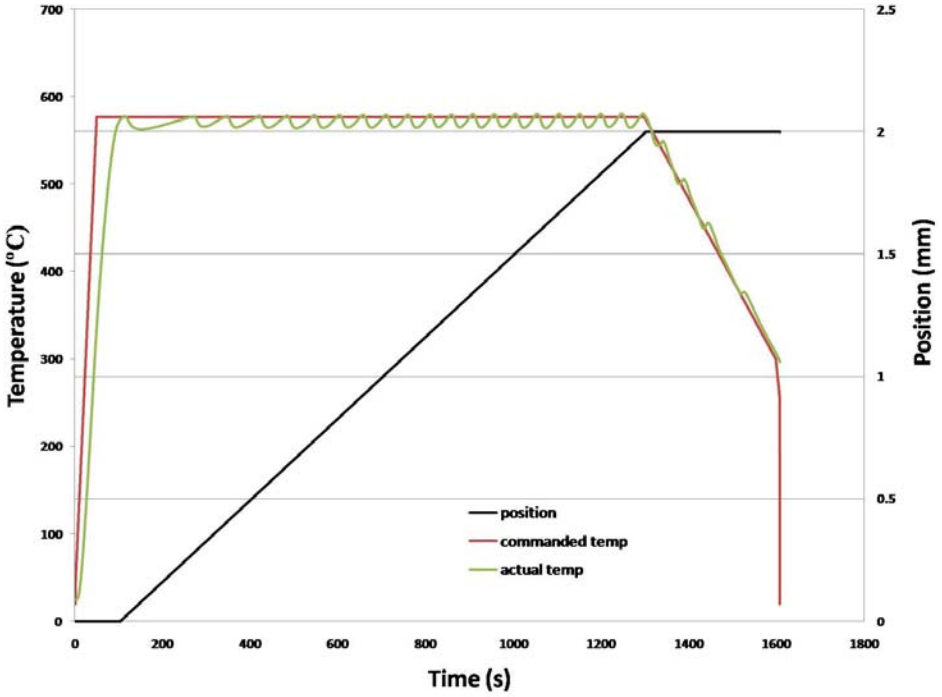

Figure 5-25: Temperature and position profile for experiments 1 and 7 in Table 5-2

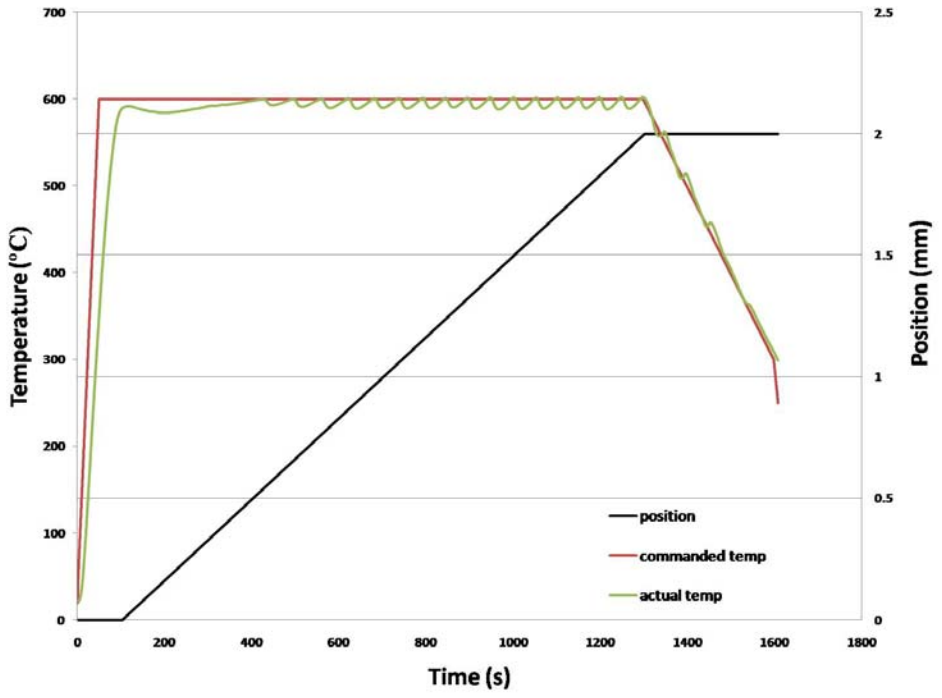

Figure 5-26: Temperature and position profile for experiments 2 and 8 in Table 5-2

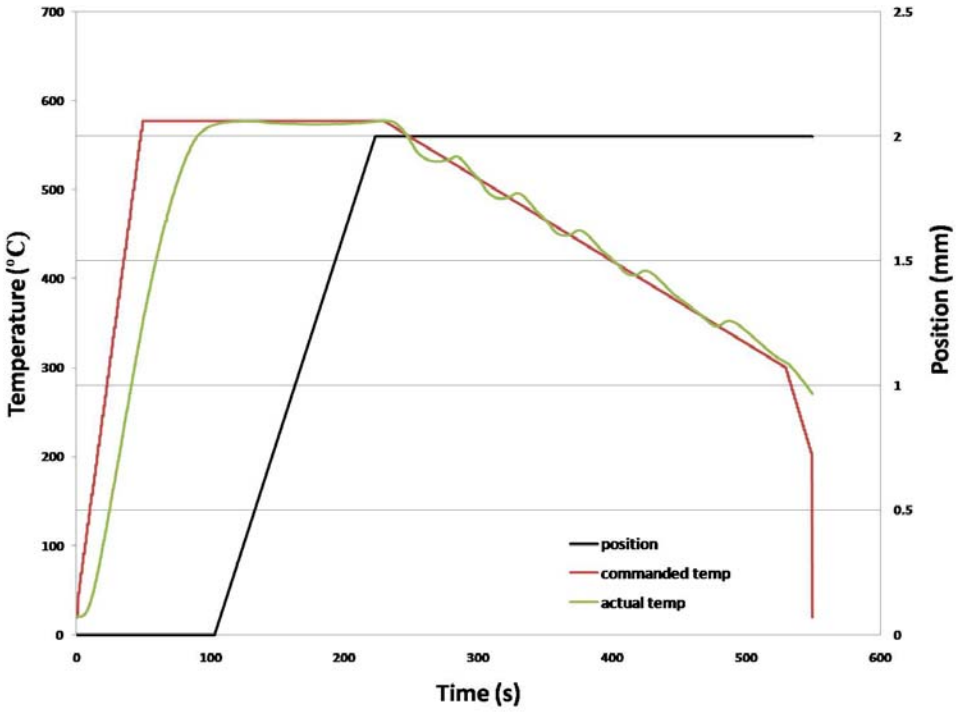

Figure 5-27: Temperature and position profile for experiments 3 and 5 in Table 5-2

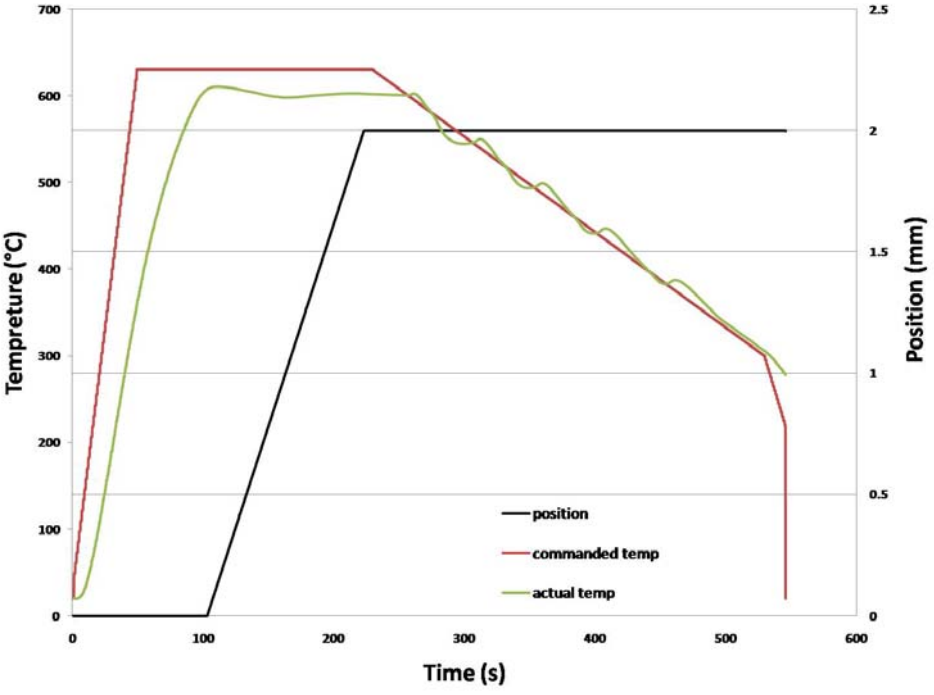

Figure 5-28: Temperature and position profile for experiments 4 and 6 in Table 5-2

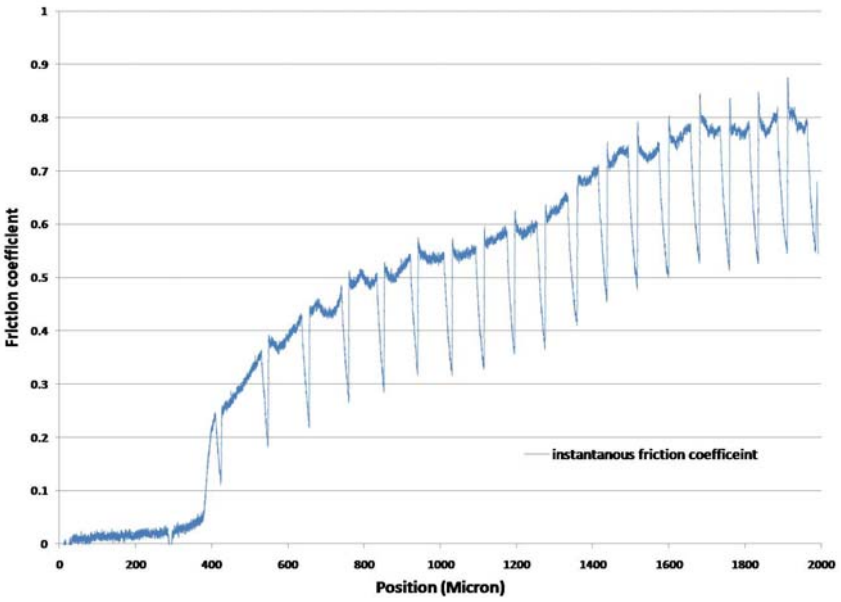

Figure 5-29: Friction coefficient versus position for experiment number 1

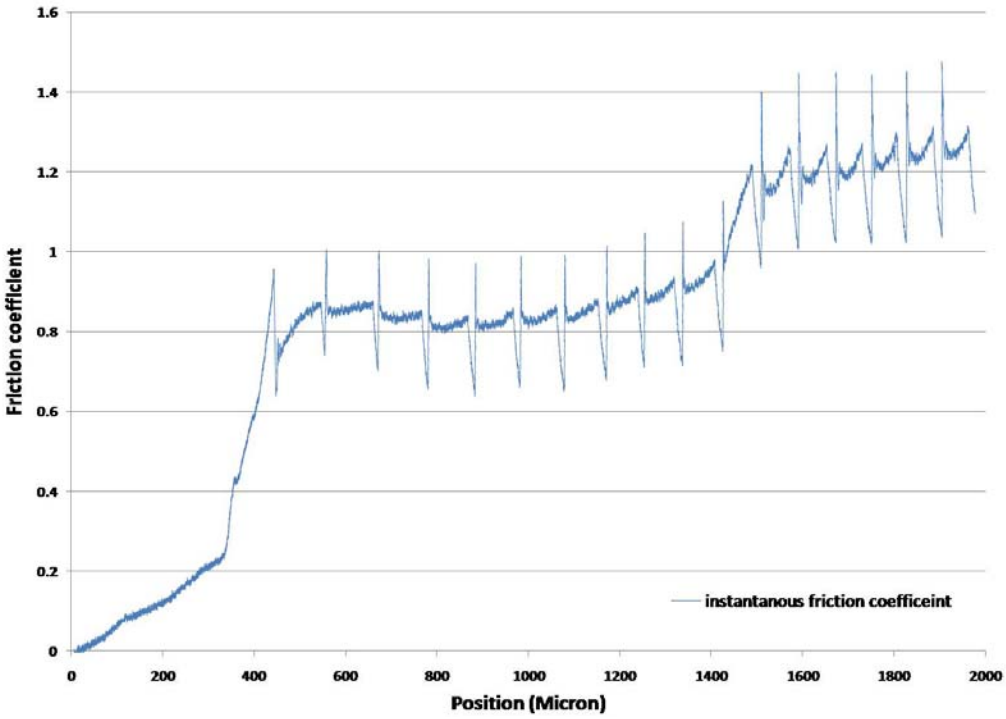

Figure 5-30: Friction coefficient versus position for experiment number 2

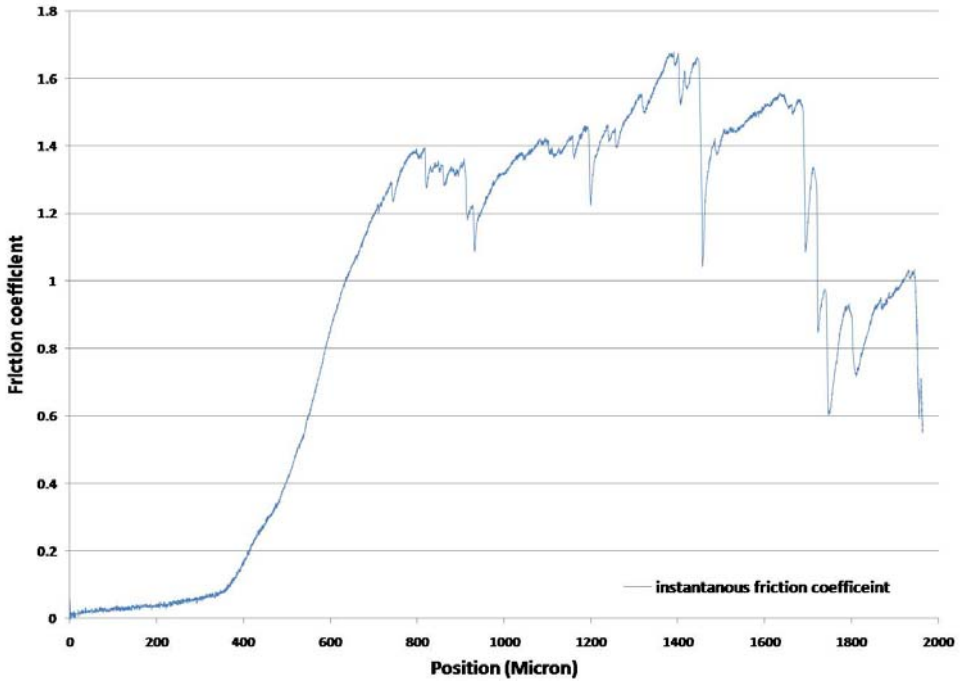

Figure 5-31: Friction coefficient versus position for experiment number 3

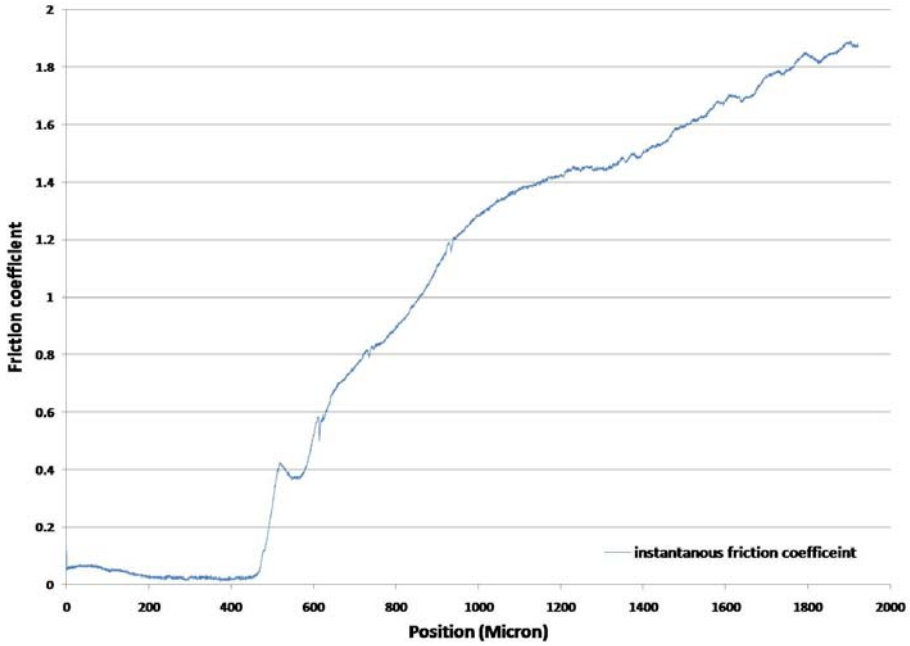

Figure 5-32: Friction coefficient versus position for experiment number 4

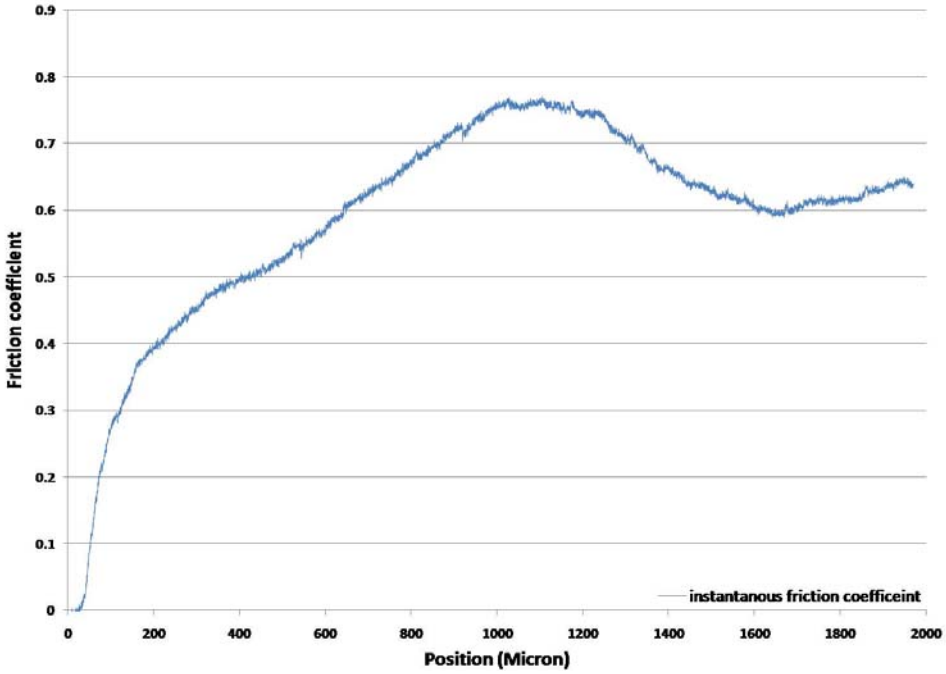

Figure 5-33: Friction coefficient versus position for experiment number 5

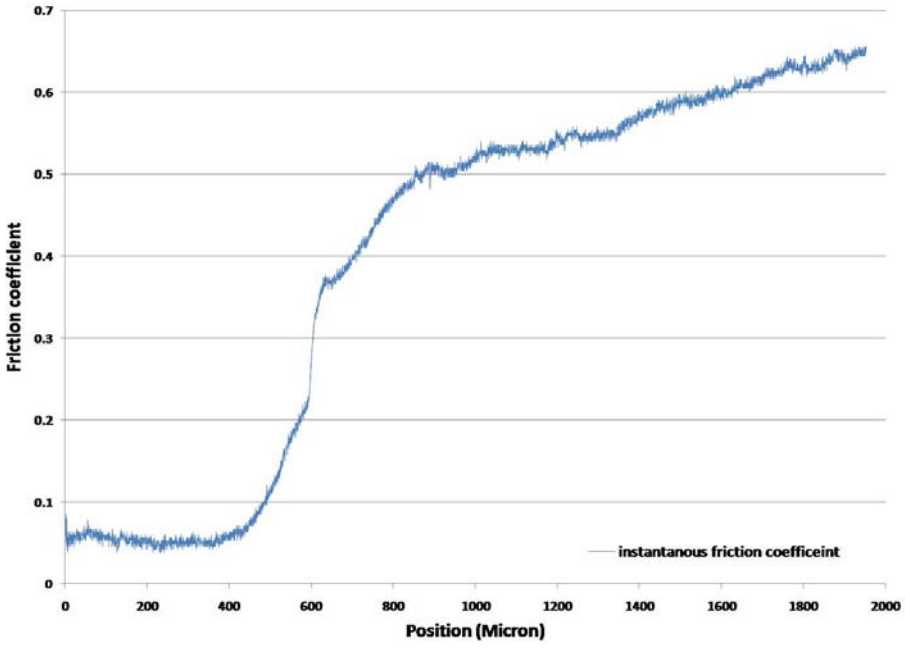

Figure 5-34: Friction coefficient versus position for experiment number 6

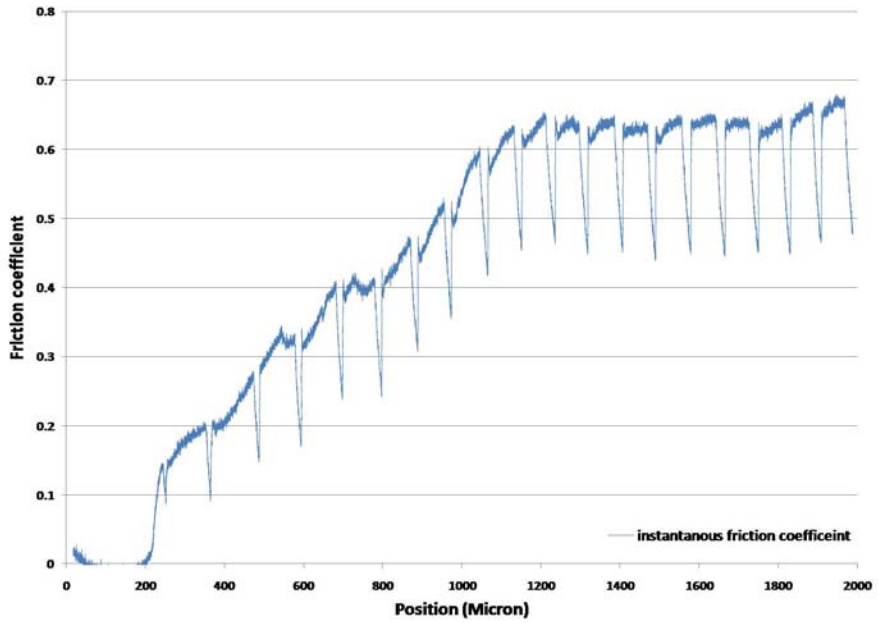

Figure 5-35: Friction coefficient versus position for experiment number 7

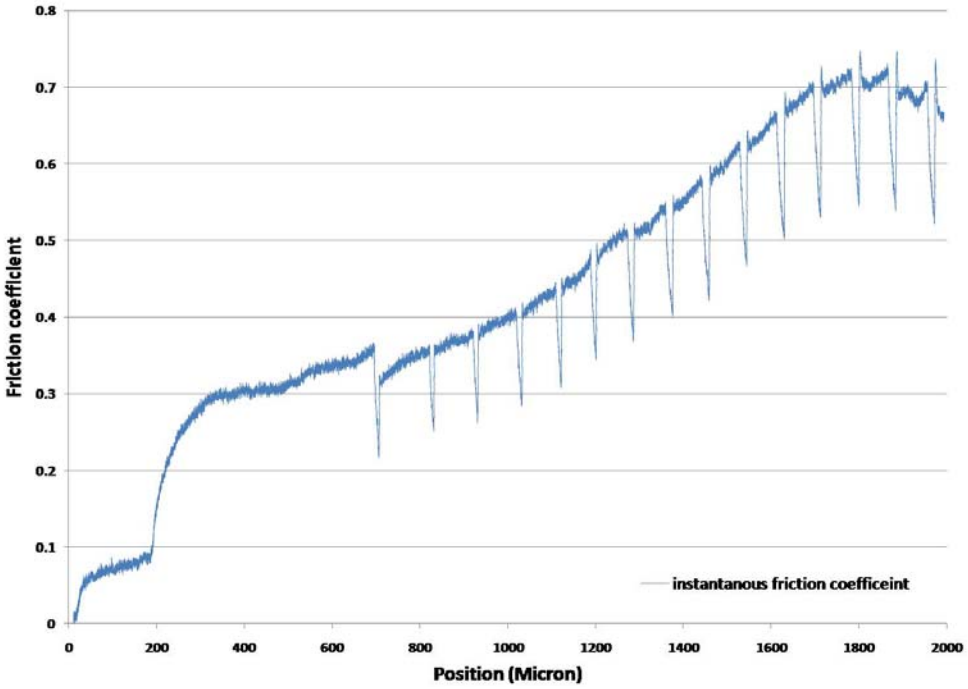

Figure 5-36: Friction coefficient versus position for experiment number 8

The experimental matrix includes four tests run at relatively slow feed rate and therefore of relatively long duration, experiments 1, 2, 7, and 8. All of these tests show a characteristic periodic fluctuation in the friction force data. These events are associated with the on-off cycles of the inductive heating system as the temperature controller attempts to regulate the temperature at the glass mold interface. When the inductive heaters shut-off, the WC mold carrier cools rapidly and shrinks in length, causing the force reading to drop rapidly. When the heaters turn on, the WC mold carrier rapidly expands to its original length and the force returns to its previous level. In our analysis of the data, we will ignore these force spikes since they are not associated with the friction behavior of the material pair, but are caused by the operation of the temperature controller.

For experiments 3, 4, 5, and 6, the feed rate is higher, resulting in tests of shorter duration and no cycling of the inductive heaters. Therefore, these tests do not show any periodic oscillation in the friction force data.

Stick-slip was not observed on any of these tests since the molds used for them have high surface finish, mold coating to prevent chemical interaction between the glass and mold surface, and are conducted in an atmosphere of UHP nitrogen.

CHAPTER SIX

OBSERVATION AND DISCUSSION

6.1 Introduction

The main objective of this research was to find the dynamic friction coefficient between a polished and coated WC mold and two types of glasses under conditions similar to the glass molding process. Moreover, finding the most significant factor in the presence of the other factors on friction measurement was another goal of this study.

Two different glasses, BK7 and soda-lime silica glass, were used in this study. These glasses have different viscosity behavior in the vicinity of their glass transition temperature, as described in Section 4.1.1; and since the friction behavior is strongly dependent on viscosity and consequently on temperature; the comparative methodology can be used to discuss the effect of different parameters.

In the following sections, the effect of different process parameters on friction coefficient for soda-lime glass is discussed. BK-7 is less suitable for understanding the effect of process parameters as its viscosity is less sensitive to temperature change.

At the end of this chapter, friction coefficient data for BK7 under process parameters similar to those used in glass molding are discussed, and the values are reported that can be used for simulation of the PGM process.

6.2 The Effect of Temperature on Friction Coefficient for Soda-Lime Glass

The actual temperature profiles for the experiments show two different families of curves. For long duration experiments the temperatures fluctuate more than short duration

experiments. Therefore, we will compare each family in its group, for example, experiment number 1 with 2 and experiment number 3 with 4.

Comparing experiments 1 and 2 shows that increasing the temperature from Tg+20 to Tg+50 has increased the friction coefficient from 0.8 to 1.2 for low feed rate (long duration) tests. Also, when comparing experiments 3 and 4 (higher feed rate) the friction coefficient increases from 1.4 to 1.8 with an increase in temperature. These experiments show that increasing temperature in the vicinity of Tg causes the friction coefficient to increase regardless of changes in other process parameters, meaning its effect dominates the other process parameters.

Finally, comparing the friction coefficients between two different glasses (first four experiments using soda lime and second four experiments using BK-7) reveals that the friction coefficient for soda lime is higher than for BK-7. This rise in amplitude is in good agreement with the results obtained in Section 5.5.5.

Any other process parameter that indirectly results in temperature change between glass and mold at the interface also can change the local viscosity of the glass and subsequently the frictional data. In the next section, the effect of mold surface roughness and normal load in relation to temperature change in the interface is discussed.

6.3 The Effect of Normal Load and Surface Roughness on Friction Coefficient for Soda-Lime

At room temperature, the friction coefficient is constant for a WC-soda lime friction pair and doesn't depend on applied load as described in Section 5.5.3. But at high temperatures, increasing the normal load increases the real area of contact between the

hot mold and glass and consequently the gap conductivity increases, meaning that there will be a better thermal path between mold and glass.

Comparing experiments 1 with 3 and 2 with 4 demonstrates that higher normal load results in an increased friction coefficient because of higher thermal conductivity at the interface. Here, the increased heat flow at the interface has decreased the viscosity of soda lime glass and consequently raised the friction coefficient. So, any process parameter that indirectly affects interface temperature may affect the viscosity and needs to be considered. For example, increasing the surface roughness has the same effect, meaning that higher surface finish can increase the interface temperature between glass and mold and subsequently increase the friction coefficient.

6.4 The Effect of Feed Rate on Friction Coefficient

The maximum temperature on the body of the friction force transducer is not more than 50ºC for long duration experiments since the high pressure nitrogen is circulating during the tests. So, the structure of the machine doesn't heat up too much and consequently the structural stiffness of the measurement loop doesn't change significantly.

Comparing experiments 1 with 3, 2 with 4, 5 with 7, and 6 with 8 shows that at high feed rates the friction coefficient rises more quickly with sliding distance than at lower feed rates. It is believed that this is due to stress relaxation in the glass. The higher feed rates provide less time for stress relaxation and the friction force rises rapidly. Conversely, at lower feed rates there is more time for stress relaxation to occur in the material and the friction force builds up more slowly. A simple calculation based on

$\tau = \eta/G$ reveals that the stress relaxation time for both glasses at Tg+50 is around 1 second, and around 4 seconds for soda lime and 12 seconds for BK7 at Tg+20. In these calculations, the shear modulus was assumed at room temperature based on data provided by supplier (Table 4-2) which is not necessarily accurate at high temperatures. The computation of the actual stress relaxation time is very difficult due to thermal gradients in the glass which cause local variations in both viscosity and shear modulus.

The feed rates used in the experimental matrix (0.1 and 1 mm/min) are smaller than the rates of typical PGM processes (2-4 mm/min). Nonetheless, we believe that a feed rate of 1 mm/min is acceptable for friction measurement at higher temperatures. At low temperatures, it is better to run the tests at lower feed rates to capture the effect of stress relaxation in friction data.

6.5 The Friction Coefficient between Polished and Coated WC-BK7 Pair at Conditions Similar to Glass Molding Process

Experiments 5 through 8 provide the friction coefficient data for BK-7 which is a typical material used in the glass molding process. Specifically, experiments 5 and 7 use process conditions similar to those used in the PGM process including molds that are coated and polished.

The friction coefficient curve for experiment number 5 shows that it ramps up to 0.75 and then levels off around 0.6 while experiment number 7 also levels off at 0.6. Comparing the results of experiment number 6 and 8 shows that the friction coefficient between BK7 and ground coated WC mold is 0.6 and 0.7, respectively.

CHAPTER SEVEN

CONCLUSION

The PGM process for molding glasses requires high pressure contact between the mold (metal) and the work piece (glass). During the molding process, the glass must move along the mold surface, either by sliding or by shear flow. At very high temperatures, the deformation very likely occurs primarily by sticking on the surface and shear flow of the material. However, at temperatures nearer to Tg, sliding frictional forces are generated at the interface between the glass/mold surfaces, and these forces affect the final shape and internal stress distribution of the molded lens. Accurate simulations of the PGM process require good models of the friction behavior at elevated temperature. The lack of such data in the literature motivated the development of the apparatus described here for experimental measurement of the friction behavior between glasses and mold materials under conditions similar to those for the PGM process.

Validation of machine functionality was conducted at room temperature for a steel-steel pair, where we found an average dynamic friction coefficient of 0.17. Using process parameters similar to the PGM process (without having Ultra High Purity nitrogen in the chamber), the experimentally reproducible static and dynamic friction coefficient was measured for a steel-BK7 pair and steel-soda lime glass pair at 577˚C. In both cases, stick-slip resulted in the dynamic friction coefficient fluctuating between 0.55 and 0.45 for BK7 and between 1.2 and 0.95 for soda lime glass. At temperatures above the glass transition temperature, Tg, which is 557˚C for BK7 and 552ºC for soda lime, the

glass exhibits a viscoelastic response to applied loads while steel is in the elastic regime. This glass viscoelasticity introduces a time dependent response to the dynamic friction data; meaning that the stick-slip response depends on the viscoelastic properties of glass at the test temperature.

Using high surface finish and coated WC molds and having Ultra High Purity nitrogen in the chamber reduced the stick-slip phenomenon in dynamic friction measurements.

An orthogonal array study, using an L8 array with five variables at two levels, was conducted for WC molds and two oxide glasses (BK7 and soda-lime-silica glass) and the important results from this study are as follows:

1- Increasing the temperature in the vicinity of Tg causes the friction coefficient to increase regardless of changes in other process parameters, meaning its effect dominates the other process parameters.

2- Higher normal load results in higher friction coefficient, presumably because of higher thermal conductivity at the interface. Also, increasing the surface roughness has the same effect, meaning that higher surface finish can increase the interface temperature between glass and mold and subsequently increases the friction coefficient.

3- Lower feed rate can give enough time for viscoelastic materials to respond to shear forces, and consequently the measured friction force rises more slowly with sliding distance.

4- Soda lime glass shows a higher friction coefficient in comparison to BK7 for the same temperature profile because of its viscosity behavior.

As a result, the friction coefficient between mold and glass in the vicinity of its transition temperature and in conditions similar to glass molding depends on temperature, feed rate, normal force, and surface roughness. Among them, temperature has the most significant effect since the glass viscosity is very sensitive to temperature.

The friction coefficient between a polished and coated WC mold and BK-7, which is a typical material for glass molding, and in conditions similar to those used in the PGM process ramps up to 0.7 and then levels off around 0.6.

CHAPTER EIGHT

FUTURE WORK

1- FEA can be used to simulate the friction between WC and glass at high temperature using the viscoelastic model of a known glass (soda-lime-silica glass). The double-sided friction test proposed in chapter 3 can be modeled by one of the friction models developed in reference [33] and then implemented in ABAQUS. This software has ability to model the glass viscoelastic properties at different temperatures. It is important to consider the equivalent structural mass and stiffness of machine at temperatures similar to real experiments and then matching the results of simulation with experiment for a known material such as soda-lime-silica glass to find the correct model of friction.

2- After finding the right friction model, sensitivity analysis with respect to material properties (Maxwell elements constants) and process parameters (temperature, normal force, strain rate) can be conducted to find the most important parameter affecting friction.

3- Comparing Figures 5-11 and 5-21 shows that both glasses (BK7 and soda lime) have different exponential stress relaxation response to same applied strain. These stress relaxation data can be used to extract the shear viscoelastic properties of glass since a thin layer of glass is under compression, meaning its bulk viscoelastic portion is small.

4- Measuring gap conductivity between polished and coated WC mold and BK7 in conditions similar to glass molding process.

REFERENCES

1. Shelby, J.E., *Introduction to Glass Science and Technology*. 2nd ed. 1997: The Royal Society of Chemistry.
2. Serope Kalpakjian, S.R.S., *Manufacturing processes for engineering materilas*. Fourth ed. 2002: Pearson Education Inc.
3. Allen Y. Yi, A.J., *Compression Molding of Aspherical Glass Lenses-A Combined Experimental and Numerical Analysis.* Journal of the American Ceramic Society, 2005. **88**(3): p. 579-586.
4. Anurag Jain, A.Y.Y., *Numerical Modeling of Viscoelastic Stress Relaxation During Glass Lens Forming Process.* Journal of the American Ceramic Society, 2005. **88**(3): p. 530-535.
5. Sellier, M., et al., *An iterative algorithm for optimal mould design in high-precision compression moulding.* Proceedings of the Institution of Mechanical Engineers, Part B: Journal of Engineering Manufacture, 2007. **221**(1): p. 25-33.
6. Klocke, F., et al., *Finite element analysis of glass moulding.* Proceedings of the Institution of Mechanical Engineers, Part B: Journal of Engineering Manufacture, 2008. **222**(1): p. 101-106.
7. AT Male, V.D., *The validity of mathematical solutions for determining friction from the ring compression test.* ASME J. Lubr. Technol., 1970. **96**: p. 482-488.
8. Sofuoglu, H., H. Gedikli, and J. Rasty, *Determination of friction coefficient by employing the ring compression test.* Journal of Engineering Materials and Technology, Transactions of the ASME, 2001. **123**(3): p. 338-348.
9. Pawelski, O., W. Rasp, and C. Hoerster, *Ring compression test as simulation test for the investigation of friction in hot metal forming.* Steel Research, 1989. 60(9): p. 395-402.
10. Wang, F. and J.G. Lenard, *An Experimental Study of Interfacial Friction-Hot Ring Compression.* Journal of Engineering Materials and Technology, 1992. **114**(1): p. 13-18.
11. Trier W., H.F., *Mechanik des Gleitens heiben, zahflussigen Glases auf Metalloberflachen.* Glastechnische Berichte, 1972. **45**(6): p. 271-276.
12. Trier W., *Gleitverhalten von heiben, zahflussigen Glas auf Metalloberflachen.* Glastechnische Berichte, 1978,. **51**(9): p. 240-243.
13. Falipou, M., F. Sicloroff, and C. Donnet, *New method for measuring the friction between hot viscous glass and metals.* Glass Science and Technology, 1999. **72**(3): p. 59-66.
14. Worgull M, H.J.F., Kabanemi K.K., Heckele M. *Characterization of Friction during the Demolding of Microstructures Molded by Hot Embossing*. in *DTIP conference*. 2006. Stresa, Italy.
15. Worgull M, K.K.K., Marcotte J.P., Hetu J.F, Heckele M. *Modeling of Large Area Hot Embossing*. in *DTIP conference*. 2007. Stresa, Italy.
16. Li, L.X., et al., *Experimental study of the lubrication behavior of A5 glass lubricant by means of the ring compression test.* Journal of Materials Processing Technology, 2000. **102**(1-3): p. 138-142.

17. Anurag Jain, A.Y.Y., *Experimental study and numerical analysis of compression molding process for manufacturing precision aspherical glass lenses*, in *School of The Ohio State University*. 2006.
18. Anurag Jain, G.C.F.A.Y.Y., *Viscosity Measurement by Cylindrical Compression for Numerical Modeling of Precision Lens Molding Process.* Journal of the American Ceramic Society, 2005. **88**(9): p. 2409-2414.
19. Http://www.nanotechsys.com/.
20. Sperling, L.H., *Introduction to physical polymer science*, ed. T. edition. 2001: John Wiley & Sons Inc.
21. Moynihan, C.T., J. Am. Ceram. Soc., 1993. **76**: p. 1081.
22. Fulcher, G.S., J. Am. Ceram. Soc., 1925. **8**(339).
23. Willian N. Findley, J.S.L., Kasif Onaran, *Creep and relaxtaion of nonlinear viscoelastic materials with an introduction to linear viscoelasticity*. 1976, Amesterdam: North-Holland publishing Company.
24. Rekhson, S.M. *Linear and non-linear viscoelasticity of glass*. 1980. Los Angeles, CA, USA.
25. Duffrene, L., et al., *Generalized Maxwell model for the viscoelastic behavior of a soda-lime-silica glass under low frequency shear loading.* Rheologica Acta, 1997. **36**(2): p. 173-86.
26. Scherer, G.W., *Relaxation in Glass and composites*. 1992: Krieger Publishing Company.
27. F. Klocke, T.B., K. Georgiadis, H. Sarikaya, F. Wang. *Coating systems for precision glass molding tools*. in *proceeding of the 7th "THE" coatings in manufacturing engineering*. 2008. Greece.
28. *The science behind material properties*. 2005.
29. Feeny, B., et al., *Historical review on dry friction and stick-slip phenomena.* Applied Mechanics Reviews, 1998. **51**(5): p. 321-341.
30. Schmitz, T.L., et al., *The difficulty of measuring low friction: uncertainty analysis for friction coefficient measurements.* Transactions of the ASME. Journal of Tribology, 2005. **127**(3): p. 673-8.
31. Grigoriev, I.S., E.Z. Meilikhov, and A.A. Radzig, *Handbook of Physical Quantities* 1997, USA: CRC Press LLC.
32. Rangnatha, S., et al., *Role of temperature on sliding response of aluminum on steel of a hot extrusion.* Materials and Manufacturing Processes, 2008. **23**(1-2): p. 29-36.
33. Persson, B.N.J., *sliding friction: physical principles and applications.* 1998: Springer.
34. T. Baumberger, F.H., B. Perrin, *Crossover from creep to inertial motion in friction dynamics.* NATURE, 1994. **367**(10 FEBRAURY): p. 544-546.
35. G. Taguchi, S.C., Y. Wu, *Taguchi's quality Engineering Handbook*. 2004: John Wiley & Sons, Inc.